

Copy
RM L53I08

NACA RM L53I08

TECH LIBRARY KAFB, NM



NACA

RESEARCH MEMORANDUM

743

AERODYNAMIC CHARACTERISTICS OF A 68.4° DELTA WING AT
MACH NUMBERS OF 1.6 AND 1.9 OVER A
WIDE REYNOLDS NUMBER RANGE

By John E. Hatch, Jr., and James J. Gallagher

Langley Aeronautical Laboratory
Langley Field, Va.

CLASSIFIED DOCUMENT

NATIONAL ADVISORY COMMITTEE
FOR AERONAUTICS

WASHINGTON

November 2, 1953

Classification cancelled (or changed to Unclassified)
By authority of 1st Lt. T. B. Amstutz (Officer making change)
G. L. O. S. E.
By
Date 10-10-68
GRADE OF OFFICER MAKING CHANGE)
1st Lt.
DATE 10-10-68

NACA RM 153108



NATIONAL ADVISORY COMMITTEE FOR AERONAUTICS

RESEARCH MEMORANDUM

AERODYNAMIC CHARACTERISTICS OF A 68.4° DELTA WING AT
MACH NUMBERS OF 1.6 AND 1.9 OVER A
WIDE REYNOLDS NUMBER RANGE

By John E. Hatch, Jr., and James J. Gallagher

SUMMARY

The results of an experimental investigation to determine the effects of Reynolds number on the aerodynamic characteristics of a 68.4° delta wing at Mach numbers of 1.6 and 1.9 are presented. The wing streamwise airfoil sections are based on the NACA 00-series with the maximum thickness varying from 4 percent at the root section to 6.24 percent at the 90-percent semispan station. At a Mach number of 1.90 force and pressure data were obtained over an angle-of-attack range of 16° at Reynolds numbers of 7.2×10^6 , 12.6×10^6 , and 18.4×10^6 . Pressure data were also obtained at Mach numbers of 1.93 and 1.62 at Reynolds numbers of 2.2×10^6 and 7.4×10^6 up to an angle of attack of 10° .

At Mach number 1.90 the force data indicated that Reynolds number had no significant effects on the measured lift and pitching moment. As the Reynolds number increased from 7.2×10^6 to 18.4×10^6 , however, the minimum drag coefficient of the wing (largely turbulent boundary layer) decreased approximately 8 percent. For the same Reynolds number range there was no change in the amount of leading-edge suction developed by the wing which was approximately 15 percent of the theoretical value.

At a given angle of attack the pressure data obtained at Mach numbers of 1.9 and 1.62 showed that an increase in Reynolds number affected the magnitude and distribution of chordwise loading but had little effect on the spanwise loading.

At both test Mach numbers the shape of the spanwise loading curve varied from elliptical at the low angles of attack to more nearly triangular at the higher angles.

INTRODUCTION

The effects of a large change in Reynolds number on the aerodynamic characteristics of a 68.4° delta wing at a Mach number of 2.41 have been reported in reference 1. The greatest effect of an increase in Reynolds number from 1.04×10^6 to 18.3×10^6 was to vary the pressure distribution over the wing upper surface at angle of attack. It was shown that an increase in Reynolds number delayed to a higher angle of attack the formation of a separated region near the wing leading edge. This region terminated in a shock wave lying approximately on a ray through the wing apex.

The purpose of the present paper is to provide further information on the effects of Reynolds number on the aerodynamic characteristics of the wing of reference 1 as well as to provide load distributions for the wing at Mach numbers of 1.6 and 1.9.

Flow-direction surveys on the wing upper surface were made in order to provide additional information on the flow phenomena over the wing.

SYMBOLS

Free-stream conditions:

M	Mach number
q_0	dynamic pressure
p_0	static pressure
R	Reynolds number, based on wing mean aerodynamic chord

Wing geometry:

A	aspect ratio
b	span
C	tangent of apex angle
c	wing chord, measured in direction of flight
\bar{c}	mean aerodynamic chord

c_{av}	average chord
S	wing area
t	thickness
α	angle of attack, deg
x	coordinate along free-stream direction
y	spanwise coordinate

Pressure data:

p	local static pressure
C_p	pressure coefficient, $\frac{p - p_0}{q_0}$
$\frac{\Delta p}{q_0 \alpha}$	lifting-surface pressure coefficient per degree angle of attack, $\frac{p_l - p_u}{q_0 \alpha}$
$\frac{c_{nc}}{c_{av}}$	span-loading coefficient, $\int_0^c \frac{C_{pl} - C_{pu}}{c_{av}} dc$
ψ	local flow angle

Force data:

C_L	wing-lift coefficient, $\frac{\text{Lift}}{q_0 S}$
C_D	wing-drag coefficient, $\frac{\text{Drag}}{q_0 S}$
C_M	wing pitching-moment coefficient about wing centroid of area, $\frac{\text{Pitching moment}}{q_0 S c}$
C_c	chord-force coefficient, $\frac{\text{Chord force}}{q_0 S}$

CONFIDENTIAL

NACA RM 153108

$$\frac{L}{D} \quad \text{lift-drag ratio}$$

$$F_s \quad \text{theoretical suction force coefficient, } \frac{C_L^2}{\pi A} \sqrt{1 - \beta^2 C^2}$$

$$\beta = \sqrt{M^2 - 1}$$

$$\Delta C_D \quad \text{incremental drag coefficient due to lift, } C_D - C_{D_{\min}}$$

Subscripts:

u conditions on wing upper surface

l conditions on wing lower surface

r value at root section

max maximum value

min minimum value

APPARATUS

Blowdown jet.- The high Reynolds number tests at $M = 1.90$ were conducted in one of the 9-inch blowdown jets of the Gas Dynamics Branch at the Langley Laboratory. The jet was so designed that the semispan models could be mounted with or without a boundary-layer scoop (fig. 1). The test section was 9 inches wide and 6 inches high when the scoop was used and 9 inches wide and 6.75 inches high when the scoop was removed.

Tunnel.- The low Reynolds number tests at $M = 1.62$ and $M = 1.93$ were conducted in the Langley 9-inch supersonic tunnel. This tunnel is a single-return, direct-drive type in which the pressure, temperature, and humidity of the enclosed air can be controlled. The semispan-wing models were mounted directly to the tunnel sidewall with no tunnel boundary-layer scoop.

Models.- The semispan-wing models having an aspect ratio of 1.57 were constructed from steel. Streamwise airfoil sections are based on the NACA 00-thickness series which has its maximum thickness at 30 percent of the chord. Leading-edge radii were modified to average about 0.4 percent of the local chord. The measured wing maximum thickness varied from

CONFIDENTIAL

4 percent at the root to 6.24 percent at the 90-percent semispan station as shown in figure 2(a). A sketch of the wing showing the locations of the pressure-survey stations is shown in figure 2(b), and the chordwise orifice locations are given in table II. Two pressure-distribution models were used in order to include the desired number of orifices, and another similar model was used for the force tests.

In order to determine the local flow direction over the wing upper surface at angles of attack, small, symmetrical, weathercocking vanes were installed on a full-span sting-mounted model in the 9-inch supersonic tunnel. Figure 3 shows the physical dimensions of the vanes as well as the vane locations on the wing surface.

TESTS AND PRECISION

The following table shows the range of the tests and the facilities used during the present investigation.

Facility	M	R	α	Data obtained
Langley 9-inch supersonic tunnel	1.62	2.2×10^6	0° to 10°	Pressure distributions
	1.62	7.2×10^6	0° to 10°	
	1.93	2.2×10^6	0° to 10°	Pressure distributions
	1.93	7.2×10^6	0° to 10°	
Blowdown jet of the Langley Gas Dynamics Branch	1.90	7.2×10^6	0° to 16°	Pressure distributions
	1.90	12.6×10^6	0° to 16°	
	1.90	18.4×10^6	0° to 16°	and forces

The wing was tested in a blowdown jet with and without a boundary-layer scoop. Force data and pressure distributions indicated practically no differences in the aerodynamic characteristics of the wing as determined by the two methods of testing. (See appendix.) The data presented for the wing, therefore, are the results obtained from the wall-mounted model with no tunnel boundary-layer scoop.

The turbulence level in the Langley 9-inch supersonic tunnel is known to be relatively low (ref. 2) and extensive laminar boundary layers are found under some conditions. In the blowdown jet, however, the turbulence level is unknown but is believed to be relatively high; this level probably results in the model boundary layers being largely turbulent for all test Reynolds numbers in this facility.

In order to understand better the direction of air flow over the wing surface, small vanes were installed at 16 different locations on the full-span model in the Langley 9-inch supersonic tunnel. The vanes were so located on the wing during each run that no interference effects between vanes were possible.

The angles through which the vanes were turned at each wing angle of attack were read by means of a cathetometer mounted outside of the tunnel. The accuracy of measurement of the indicated flow angles is estimated at $\pm \frac{1}{2}^{\circ}$. Additional information on the direction of flow in the boundary layer was obtained by an ink-flow method. Ink was allowed to issue from the wing surface through static orifices located in the wing, and the path of the ink taken in the boundary layer was photographed.

The estimated probable errors in the aerodynamic coefficients are as follows:

R	C_p	C_L	C_D	C_M	C_c ($\alpha = 0$)
2.2×10^6	± 0.0050	-----	-----	-----	-----
7.2×10^6	± 0.0015	± 0.0020	± 0.0006	± 0.0006	± 0.0002
12.6×10^6	± 0.0030	± 0.0010	± 0.0003	± 0.0003	± 0.0001
18.4×10^6	± 0.0020	± 0.0020	± 0.0003	± 0.0003	± 0.0001

Calibration of the tunnel shows the Mach number to be 1.62 ± 0.01 and 1.93 ± 0.015 . For the blowdown jet the Mach number was 1.90 ± 0.015 . The probable error in angle of attack in referencing the models was $\pm 0.07^{\circ}$ with respect to the tunnel center line and $\pm 0.03^{\circ}$ in relative angle of attack.

RESULTS AND DISCUSSION

Force Data

The force data were obtained only with the semispan model in the blowdown jet at $M = 1.90$. Data are presented in figure 4 at Reynolds numbers of 7.2×10^6 and 18.4×10^6 based on the mean aerodynamic chord. Force data taken at a $R = 12.6 \times 10^6$ were the same as those obtained at $R = 18.4 \times 10^6$ and, therefore, are not presented.

Lift.- No significant effects within the experimental accuracy can be noted on the lift throughout the range of Reynolds numbers tested. The lift-curve slope is linear up to about an angle of attack of 8° where the slope begins to decrease because of separation effects. For the low angles of attack the slope of the lift curve was 0.0290 per degree compared to the value of 0.033 as obtained from theory in reference 3.

Drag.- The only significant change in the drag data with Reynolds number was a variation of $C_{D_{min}}$. A value of $C_{D_{min}}$ of 0.0094 was obtained at a Reynolds number of 7.2×10^6 and decreased to 0.0086 at a Reynolds number of 18.4×10^6 . Up to about an angle of attack of 8° a slight decrease in drag coefficient with increasing Reynolds number may also be noted. It is believed that the wing boundary layer is almost entirely turbulent at the test Reynolds numbers, and a decrease of this order of magnitude in drag coefficient is to be expected with increasing Reynolds number.

Integration of the pressure distributions obtained at a Reynolds number of 18.4×10^6 (fig. 5) gives a value of 0.0051 for the pressure drag coefficient for this wing. When the pressure drag coefficient is subtracted from $C_{D_{min}}$ for the wing mounted on the sidewall, a value of 0.0035 for the skin-friction coefficient is obtained at a Reynolds number of 18.4×10^6 . For the wing in the presence of the boundary-layer scoop the skin-friction coefficient was found to be 0.0040. For a flat plate at the same Reynolds number, reference 4 gives an experimental value of 0.0044 for the turbulent skin-friction coefficient; this value compares favorably with that obtained for the wing.

Lift-drag ratio.- A value of 7.2 for $(L/D)_{max}$ is obtained at the highest Reynolds number. This value decreases slightly with decreasing Reynolds number; this decrease is due in part to the increase in skin friction obtained at the lower Reynolds numbers.

Pitching moment.- The only discernible Reynolds number effects appear in the pitching moment although even these are small. Figure 4 shows that at the higher angles of attack the center of pressure of the wing moves forward slightly with increasing Reynolds number. The shift amounts to a forward movement of the center of pressure of about only 1 percent of the mean aerodynamic chord at an angle of attack of 16° . The reversal in slope in the moment curve at about an angle of attack of 8° coincides with the point at which the lift-curve slope begins to decrease.

Leading-edge suction.- The linearized theory predicts that a suction force is developed on round-nose airfoils at supersonic speeds when the leading edge of the airfoil is swept behind the Mach cone. When the value

of the drag-rise factor $\Delta C_D/C_L^2$ is less than the reciprocal of the lift-curve slope, a suction force is developed which indicates that the resultant lift vector is tilted forward. Experimentally, a decrease in skin friction with increasing angle of attack would also show the same effect. Since it is not possible to isolate completely the skin-friction effects on the drag-rise factor, the concept of leading-edge suction should be used only as a convenient method of comparing the relative merits of different wings.

Figure 6 shows the experimental variation of ΔC_D with C_L^2 as well as the theoretical curve assuming the wing to be developing full leading-edge suction. Only about 15 percent of the theoretical suction force was indicated. Although the data are not shown, a change in Reynolds number from 7.2×10^6 to 18.4×10^6 had no effect on the leading-edge suction for this wing. Figure 7 is presented in order to show more clearly the little drag relief that was obtained. The theoretical chord-force coefficient, assuming the wing to be developing full leading-edge suction, was calculated by the method of reference 2 by using the theoretical lift-curve slope for the wing. The theoretical curve if extended indicates that the wing would actually have a negative value of chord-force coefficient at an angle of attack above 5° if full suction were attained. Actually, of course, the leading-edge-suction force is limited to some value of pressure close to vacuum acting on a small area along the leading edge. The experimental curve does show a decrease in C_c but it is nowhere near the order predicted by theory.

FLOW STUDIES

An examination of the pressure data indicated that the character of the flow over the wing is, in general, the same at $M = 1.6$ and 1.9 as it was at $M = 2.41$ (ref. 1). Pressure discontinuities on the wing upper surface show that standing shock waves exist at each of the test Mach numbers. For example, figure 8 shows the spanwise variation of upper-surface pressure coefficients at the 90-percent root-chord station for a wing angle of attack of 10° at $M = 1.9$. The data at each Reynolds number indicate that a separated region exists near the leading edge and is followed by an abrupt change in pressure which usually denotes the presence of a shock wave. From additional spanwise pressure plots, the shock wave was found to lie along a ray through the wing apex.

A flow-direction survey was made just above the wing surface by means of weathercocking vanes placed on the full-span wing. In addition, the flow direction in the boundary layer was observed by means of an ink-flow technique. From the results of the vane survey, it was found that outboard

of the shock wave lying along a ray through the wing apex the flow was toward the root chord, whereas, behind the shock wave, the flow was approximately parallel to the root chord. Figure 9 shows some results of the flow-direction survey made at the 70-percent root chord station. At $M = 1.62$ and $M = 1.93$, the local flow angles increased with increasing angle of attack. It should be noted that the abrupt change in the indicated flow angles occurs at the location of the shock wave on the wing surface as determined from the pressure distributions. Complete results of the vane survey are presented in table I.

The flow direction in the boundary layer was observed at $M = 1.93$ in the Langley 9-inch supersonic tunnel over an angle-of-attack range as the Reynolds number varied from 1.3×10^6 to 5×10^6 . Ink was admitted at several points on the full-span wing upper surface and the resulting flow patterns were photographed as the angle of attack and Reynolds number were varied. Figure 10 shows some results of the ink-flow studies obtained at a Reynolds number of 1.3×10^6 over an angle-of-attack range. With the wing at an angle of attack of 0° the ink flowed approximately parallel to the stream direction, but, as the angle of attack increased, the ink showed that the boundary-layer flow at the wing surface was turned outboard and toward the tip. The ink-flow pictures as well as the pressure data show that separation begins at the tip and moves toward the wing apex with increasing angle of attack. Combining the results of pressure distributions, vane surveys, and the ink-flow photographs led to the conclusion that the flow configuration was probably as shown in figure 11. A lambda shock occurred on the wing with the front leg starting at the point of laminar separation and the back leg originating along the line of flow reattachment. Between the two legs of the lambda shock the flow direction was outboard on the wing surface and inboard a small distance above the surface. Behind the back leg of the lambda shock the flow just above the surface is approximately parallel to the stream direction as shown by the vane survey. Similar wing-shock configurations were photographed and reported in reference 5.

Pressure data obtained at a Reynolds number of 18.4×10^6 show that up to an angle of attack of 16° (the limit of the present tests) the back leg of the lambda shock moves inboard and the leading-edge separation continues to move toward the wing apex with increasing angle of attack.

Figure 12 shows some ink-flow pictures for the wing at an angle of attack of 2° as the Reynolds number was varied from 1.3×10^6 to 5×10^6 at $M = 1.93$. At a Reynolds number of 1.3×10^6 , the ink-flow photographs indicate that separation has started near the tip as evidenced by the ink flowing along the leading edge. As the Reynolds number is increased the point of leading-edge separation moves toward the tip until finally the ink spreads out over the wing surface and then flows in the stream direction

which shows that the flow is no longer separated. The pressure-distribution data also indicate that an increase in Reynolds number delays the leading-edge separation to a higher angle of attack.

LOADING

It has been shown that an increase in test Reynolds number changes the flow over the wing. It will, therefore, be of interest to determine the effect that Reynolds number has on the wing loading coefficients. Only representative data which show the effects of Reynolds number are plotted in this paper. Complete pressure data for the wing at $M = 1.62$ and $M = 1.9$ are presented in tables II and III.

Figure 13(a) shows the chordwise variation of loading coefficients for the wing at $M = 1.9$ and $\alpha = 6^\circ$ for Reynolds numbers of 2.2×10^6 and 18.4×10^6 . At the 11.1-percent semispan station there is little effect of Reynolds number on the loading, but in moving outboard the distribution and magnitude of the chordwise loading coefficients change with Reynolds number. For example, at the 77.7-percent semispan station the higher Reynolds number tests result in loading coefficients on the order of 15 to 20 percent higher than those obtained at a Reynolds number of 2.2×10^6 . The agreement between experiment and theory is good at the inboard station, but becomes progressively worse in moving outboard owing to flow separation which begins at the tip. As a result of flow separation the loading over the three outboard stations is not linear with angle of attack. The variation in loading at the inboard station, however, is nearly linear over the entire test range.

It was found that the greatest changes in loading coefficients occurred as the Reynolds number was increased from 2.2×10^6 to 7.2×10^6 . As the Reynolds number was further increased to 18.4×10^6 the loading continued to vary but the changes in loading over that obtained at a Reynolds number 7.2×10^6 were small. As the angle of attack increased above 6° the effects of Reynolds number on the chordwise loading coefficients decreased. The pressure data indicate that at about an angle of attack of 14° Reynolds number will have little effect on the loading coefficients since the flow has separated over most of the wing even at a Reynolds number of 18.4×10^6 . The pressure-distribution data obtained at a Reynolds number of 7.2×10^6 in the Langley 9-inch supersonic tunnel at angles of attack up to 10° (the limit of the tunnel tests) were in good agreement with those data (not presented) for the wing at the same Reynolds number in the blowdown jet.

As shown by figure 13(b) the same general changes in wing loading occurred with Reynolds number at $M = 1.62$ as occurred at $M = 1.9$. Even though the highest test Reynolds number at $M = 1.62$ was 7.2×10^6 it is believed that the loading coefficients presented are approximately the same as would be obtained at higher Reynolds numbers since at $M = 1.9$ and $M = 2.41$ an increase in Reynolds number above 7.2×10^6 had little effect on the wing loading coefficients.

Figure 13 illustrated that Reynolds number had significant effects on the distribution and magnitude of chordwise loading coefficients. It is important, then, to examine the effects of Reynolds number on the spanwise loading which was obtained from the integrated pressure distributions at each chordwise station.

Figure 14(a) shows the variation in experimental loading across the span for the wing at angles of attack of 6° , 10° , and 16° at $M = 1.9$. It may be seen that the effects of Reynolds number on the spanwise loading are small. At an angle of attack of 6° , for example, the integrated data obtained at a Reynolds number of 18.4×10^6 result in a lift coefficient approximately 4 percent higher than the lift coefficient obtained at a Reynolds number of 2.2×10^6 . The experimental data and theory show good agreement at an angle of attack of 6° . As the angle of attack increases to 16° the shape of the span-loading curve changes from near elliptical to approximately a triangular distribution. Figure 14(b) shows that the span loadings at $M = 1.62$ also follow the same trends.

CONCLUSIONS

From the experimental investigation to determine the effects of Reynolds number on the aerodynamic characteristics of a delta wing the following conclusions may be drawn:

1. Over an angle-of-attack range of 0° to 16° at Mach number 1.90 the only significant effect of a Reynolds number change from 7.2×10^6 to 18.4×10^6 on the measured force data was to decrease the wing minimum drag coefficient about 8 percent.
2. At Mach number 1.90, there was no effect of a Reynolds number increase from 7.2×10^6 to 18.4×10^6 on the amount of leading-edge suction developed by the wing which was approximately 15 percent of the theoretical value.

~~CONFIDENTIAL~~

NACA RM L53I08

3. At Mach numbers 1.62 and 1.9, a large increase in Reynolds number definitely affected the magnitude and distribution of chordwise loading but had little effect on the resultant spanwise loading.

4. The shape of the spanwise loading curve varied from elliptical at the low angles of attack to more nearly triangular at the higher angles.

5. With the semispan wing mounted directly to the tunnel side wall at Mach numbers 1.90 and 2.41, the wing aerodynamic characteristics were the same as those obtained with the wing tested in the presence of a tunnel boundary-layer scoop for Reynolds numbers of 12.6×10^6 and 18.4×10^6 .

Langley Aeronautical Laboratory,
National Advisory Committee for Aeronautics,
Langley Field, Va., August 25, 1953.

~~CONFIDENTIAL~~

APPENDIX

The use of a boundary-layer scoop exhausting to the atmosphere presents several problems. For example, the scoop will not start at low stagnation pressure which, of course, means that low Reynolds number tests cannot be made. In addition, a disturbance which is not always easily eliminated originates from the scoop-tunnel-wall juncture. It would be desirable and convenient, therefore, to conduct tests at supersonic speeds without a boundary-layer scoop if the test results would not be adversely affected.

During the present investigation, the effects of testing a 68.4° delta wing with and without a boundary-layer scoop were determined. The ratio of the tunnel boundary-layer thickness to wing semispan was about 1/10 when the wing was tested without the boundary-layer scoop.

Force test. - Figure 15 shows force data obtained at $M = 1.90$ and $M = 2.41$ for the wing tested with and without a boundary-layer scoop. Up to an angle of attack of 16° (the limit of the present tests), the only significant effect on the measured force coefficients of testing the wing mounted directly to the side wall was to lower the minimum drag coefficient approximately 3 to 5 percent. A small decrease in drag coefficient is to be expected since part of the wing was immersed in the tunnel boundary layer. At $M = 2.41$ there was a slight rearward shift in the wing center-of-pressure location when the wing was tested without a boundary-layer scoop in place. At an angle of attack of 16° the rearward center-of-pressure shift was about 1 percent of the mean aerodynamic chord.

Pressure data. - For the no-scoop condition, if the tunnel boundary layer were to influence the pressure distribution over the wing, the pressures at the inboard stations would be most affected. Figure 16 presents representative plots of pressure coefficients at the 11.1-percent semispan station for $M = 1.9$ and a Reynolds number of 18.4×10^6 . Figure 16 shows that the pressure data obtained by the two methods of testing are the same. The agreement shown at the inboard station is typical of the pressure distributions at the other spanwise stations over the test angle-of-attack range of 0° to 16° .

Figure 17 shows some typical pressure distributions at $M = 2.41$ for the 11.1-percent and 33.3-percent semispan stations. At the 11.1-percent semispan station the pressures show some disagreement over the forward 40 percent of the airfoil between the two methods of testing. At angles of attack, the scoop tests result in slightly higher negative pressures on the upper surface than do the no-scoop tests. The trends, which occurred at $\alpha = 8^\circ$, continued to the higher angles of attack, but the agreement was somewhat improved at the higher angles.

At the 33.3-percent semispan station the pressures obtained show good agreement over the forward 60 percent of the airfoil at $\alpha = 0^\circ$, but over the remainder of the airfoil the scoop tests again result in higher negative pressures than those pressures obtained without the boundary-layer scoop. When the angle of attack is increased to 8° , no differences in the pressure distributions are noticeable. The pressures obtained at the 55.5-percent and the 77.7-percent semispan stations were the same for both methods of testing over the angle-of-attack range of 0° to 16° .

It may be seen, therefore, that the no-scoop tests result in local decreases in lifting pressures on the order to 5 percent below the pressures obtained with a scoop-mounted model. The local reductions in lift are also apparent in the force data which indicated a slight rearward shift in the center of pressure for the no-scoop tests.

The results of the present tests indicate that, when testing highly sweptback wings at Mach numbers of about 2 and Reynolds numbers of 12×10^6 , if the ratio of tunnel-boundary-layer thickness to wing semispan is of the order of 1/10, correct over-all aerodynamic characteristics can be obtained by mounting the model directly to the tunnel sidewall. Local lifting pressures over inboard stations, however, can be in error approximately 5 percent at low angles of attack.

[REDACTED]
REFERENCES

1. Hatch, John E., Jr., and Hargrave, L. Keith: Effects of Reynolds Number on the Aerodynamic Characteristics of a Delta Wing at Mach Number of 2.41. NACA RM L51H06, 1951.
2. Love, Eugene S., Coletti, Donald E., and Bromm, August F., Jr.: Investigation of the Variation With Reynolds Number of the Base, Wave, and Skin-Friction Drag of a Parabolic Body of Revolution (NACA RM-10) at Mach Numbers of 1.62, 1.93, and 2.41 in Langley 9-Inch Supersonic Tunnel. NACA RM L52H21, 1952.
3. Brown, Clinton E.: Theoretical Lift and Drag of Thin Triangular Wings at Supersonic Speeds. NACA Rep. 839, 1946. (Supersedes NACA TN 1183.)
4. Wilson, R. E., Young, E. C., and Thompson, M. J.: 2nd Interim Report on Experimentally Determined Turbulent Boundary-Layer Characteristics at Supersonic Speeds. CM 501 (ut/IRL 196), Contract N0rd-9195, Bur. Ord., Univ. Texas, Defense Res. Lab. The Johns Hopkins Univ. Appl. Phys. Lab., Jan. 25, 1949.
5. Love, Eugene S., and Grigsby, Carl E.: A New Shadowgraph Technique for the Observation of Conical Flow Phenomena in Supersonic Flow and Preliminary Results Obtained for a Triangular Wing. NACA TN 2950, 1953.

[REDACTED]

[REDACTED]

CONFIDENTIAL

TABLE I

MEASURED LOCAL FLOW ANGLES

[All angles in degrees]

$$M = 1.93, \quad R = 1.3 \times 10^6$$

Vane no.	α	0°	2°	4°	6°	8°	10°
1	0.1	0.5	0.6	1.0	0.9	1.1	
2	-.4	.5	1.5	2.6	3.5	4.9	
3	-1.0	-.2	1.7	4.0	5.9	8.5	
4	1.3	1.9	2.8	3.0	3.0	4.0	
5	1.0	2.0	3.2	4.3	5.3	7.8	
6	.9	2.7	4.4	7.3	10.8	13.5	
7	1.0	.9	1.4	1.6	1.6	1.1	
8	.5	1.1	1.6	2.1	2.2	1.8	
9	1.1	1.4	1.7	2.5	2.9	3.8	
10	1.1	2.2	4.1	4.0	6.6	13.2	
11	1.6	3.0	5.5	6.7	11.2	16.6	
12	1.6	3.5	5.8	9.7	13.5	16.4	
13	1.5	3.5	6.0	10.1	13.9	16.6	
14	-.5	.1	.5	.8	.3	-.2	
15	1.0	2.5	3.6	4.5	9.0	14.0	
16	2.1	5.0	8.3	13.1	15.8	18.3	

$$M = 1.62, \quad R = 1.4 \times 10^6$$

Vane no.	α	0°	2°	4°	6°	8°	10°
1		0.8	1.2	1.8	2.1	2.6	3.1
2		.4	1.2	2.1	3.1	3.9	4.9
3		-.8	.6	2.0	4.3	5.7	8.5
4		1.7	2.4	2.5	3.0	4.1	3.6
5		2.0	3.0	4.0	4.7	5.2	7.5
6		.9	2.9	5.2	7.9	11.7	15.6
7		.4	.5	.9	1.5	1.9	.4
8		1.6	2.3	2.5	2.9	2.7	3.0
9		1.6	2.0	3.0	3.4	3.0	2.3
10		2.0	2.9	3.7	4.8	6.5	9.9
11		1.6	2.8	3.8	5.0	7.6	14.8
12		1.2	2.6	5.2	5.8	11.3	18.7
13		1.7	3.8	7.2	10.1	16.1	20.6
14		-.1	0	.7	1.1	2.0	.8
15		.8	1.2	2.3	2.7	1.7	7.7
16		2.6	5.1	6.9	11.1	20.3	10.2

TABLE II-- EXPERIMENTAL PRESSURE COEFFICIENTS
 $Re = 15.4 \times 10^6$
 $\mathbf{M} = 1.90$

Station		$\alpha = 0^\circ$		$\alpha = 2^\circ$		$\alpha = 4^\circ$		$\alpha = 6^\circ$		$\alpha = 8^\circ$		$\alpha = 10^\circ$		$\alpha = 12^\circ$		$\alpha = 14^\circ$		
y	$b/2$	c_p	c_{p_u}	c_{p_l}	c_{p_u}	c_{p_l}	c_{p_u}	c_{p_l}	c_{p_u}	c_{p_l}								
0.1111	0	0.218	0.206	0.215	0.176	0.197	0.145	0.168	0.109	0.127	0.079	0.082	0.058	0.054	0.043	-0.020	0.030	-0.057
	3.8	0.045	-0.006	-0.081	-0.037	-0.120	-0.085	-0.155	-0.101	-0.121	-0.147	-0.214	-0.214	-0.201	-0.209	-0.228	-0.303	-0.360
	7.3	0.023	-0.011	-0.063	-0.047	-0.098	-0.079	-0.134	-0.111	-0.123	-0.150	-0.210	-0.186	-0.202	-0.236	-0.299	-0.379	-0.416
	10.6	0.008	-0.023	-0.038	-0.051	-0.071	-0.065	-0.103	-0.093	-0.103	-0.129	-0.182	-0.156	-0.221	-0.233	-0.267	-0.382	-0.411
	14.2	-0.003	-0.026	-0.051	-0.051	-0.057	-0.073	-0.091	-0.086	-0.092	-0.119	-0.168	-0.140	-0.199	-0.200	-0.251	-0.382	-0.405
	17.5	-0.008	-0.028	-0.041	-0.053	-0.073	-0.073	-0.085	-0.082	-0.092	-0.118	-0.158	-0.130	-0.191	-0.197	-0.236	-0.376	-0.405
	21.2	-0.011	-0.032	-0.046	-0.053	-0.063	-0.073	-0.073	-0.080	-0.086	-0.110	-0.134	-0.125	-0.185	-0.173	-0.214	-0.313	-0.354
	24.7	-0.007	-0.026	-0.048	-0.065	-0.065	-0.075	-0.087	-0.088	-0.098	-0.104	-0.138	-0.110	-0.176	-0.180	-0.216	-0.315	-0.356
	28.2	-0.007	-0.027	-0.029	-0.047	-0.066	-0.066	-0.078	-0.085	-0.093	-0.103	-0.139	-0.117	-0.176	-0.183	-0.217	-0.316	-0.357
	31.7	-0.009	-0.028	-0.035	-0.048	-0.063	-0.066	-0.070	-0.089	-0.090	-0.102	-0.133	-0.119	-0.179	-0.180	-0.217	-0.316	-0.350
	36.2	-0.016	-0.026	-0.038	-0.033	-0.072	-0.061	-0.090	-0.092	-0.098	-0.107	-0.137	-0.123	-0.159	-0.160	-0.200	-0.318	-0.351
	41.7	-0.022	-0.041	-0.048	-0.061	-0.077	-0.073	-0.086	-0.092	-0.098	-0.115	-0.155	-0.134	-0.192	-0.190	-0.233	-0.353	-0.370
	46.2	-0.035	-0.051	-0.059	-0.066	-0.086	-0.086	-0.098	-0.098	-0.102	-0.114	-0.150	-0.130	-0.188	-0.186	-0.217	-0.358	-0.375
	51.0	-0.028	-0.047	-0.055	-0.066	-0.080	-0.086	-0.096	-0.096	-0.102	-0.113	-0.153	-0.133	-0.186	-0.186	-0.216	-0.359	-0.379
	56.7	-0.031	-0.049	-0.077	-0.069	-0.071	-0.083	-0.095	-0.099	-0.102	-0.115	-0.156	-0.132	-0.188	-0.177	-0.220	-0.363	-0.380
	64.3	-0.032	-0.050	-0.068	-0.069	-0.076	-0.085	-0.095	-0.099	-0.102	-0.115	-0.156	-0.132	-0.189	-0.180	-0.216	-0.361	-0.375
	71.7	-0.034	-0.051	-0.068	-0.069	-0.076	-0.083	-0.093	-0.099	-0.101	-0.115	-0.156	-0.131	-0.195	-0.177	-0.216	-0.361	-0.377
	77.5	-0.036	-0.052	-0.069	-0.070	-0.081	-0.081	-0.094	-0.098	-0.101	-0.116	-0.158	-0.133	-0.196	-0.175	-0.215	-0.365	-0.375
	83.2	-0.037	-0.055	-0.071	-0.073	-0.080	-0.087	-0.095	-0.101	-0.106	-0.118	-0.160	-0.130	-0.198	-0.180	-0.216	-0.366	-0.370
	88.7	-0.046	-0.055	-0.080	-0.071	-0.084	-0.087	-0.098	-0.101	-0.102	-0.119	-0.168	-0.135	-0.196	-0.182	-0.213	-0.363	-0.371
	94.0	-0.048	-0.071	-0.068	-0.092	-0.093	-0.103	-0.097	-0.118	-0.109	-0.130	-0.168	-0.155	-0.193	-0.167	-0.212	-0.364	-0.374
0.3333	0	-1.71	-1.33	-1.67	-0.68	-1.71	0	-1.43	-0.68	-1.01	-1.05	-0.66	-1.36	-0.91	-1.65	0	-1.97	-0.038
	4.8	-0.049	-0.149	-0.04	-0.142	-0.111	-0.167	-0.152	-0.250	-0.193	-0.285	-0.228	-0.333	-0.261	-0.298	-0.311	-0.333	-0.333
	9.2	-0.065	-0.070	-0.023	-0.137	-0.065	-0.210	-0.107	-0.271	-0.149	-0.293	-0.187	-0.313	-0.228	-0.273	-0.289	-0.324	-0.312
	14.2	-0.033	-0.070	-0.048	-0.114	-0.066	-0.144	-0.086	-0.249	-0.147	-0.293	-0.178	-0.323	-0.208	-0.273	-0.282	-0.319	-0.296
	18.7	-0.035	-0.069	-0.038	-0.108	-0.071	-0.148	-0.076	-0.201	-0.135	-0.249	-0.159	-0.283	-0.194	-0.218	-0.232	-0.286	-0.266
	23.2	-0.037	-0.067	-0.033	-0.100	-0.071	-0.142	-0.066	-0.189	-0.136	-0.246	-0.153	-0.289	-0.184	-0.218	-0.227	-0.284	-0.272
	28.2	-0.038	-0.063	-0.034	-0.093	-0.074	-0.121	-0.062	-0.175	-0.129	-0.239	-0.156	-0.285	-0.186	-0.216	-0.227	-0.284	-0.261
	32.7	-0.037	-0.062	-0.036	-0.090	-0.074	-0.115	-0.057	-0.176	-0.128	-0.238	-0.156	-0.285	-0.185	-0.215	-0.226	-0.283	-0.257
	40.3	-0.045	-0.070	-0.031	-0.096	-0.088	-0.105	-0.058	-0.182	-0.133	-0.241	-0.160	-0.291	-0.191	-0.221	-0.230	-0.289	-0.270
	47.5	-0.047	-0.066	-0.023	-0.087	-0.093	-0.106	-0.058	-0.177	-0.137	-0.238	-0.161	-0.286	-0.191	-0.220	-0.230	-0.288	-0.264
	53.0	-0.047	-0.067	-0.021	-0.087	-0.093	-0.105	-0.058	-0.177	-0.137	-0.238	-0.161	-0.286	-0.191	-0.220	-0.230	-0.288	-0.264
	58.2	-0.047	-0.067	-0.021	-0.087	-0.093	-0.105	-0.058	-0.177	-0.137	-0.238	-0.161	-0.286	-0.191	-0.220	-0.230	-0.288	-0.264
	63.7	-0.047	-0.067	-0.021	-0.087	-0.093	-0.105	-0.058	-0.177	-0.137	-0.238	-0.161	-0.286	-0.191	-0.220	-0.230	-0.288	-0.264
	70.2	-0.048	-0.068	-0.023	-0.087	-0.094	-0.106	-0.058	-0.178	-0.138	-0.239	-0.162	-0.287	-0.192	-0.221	-0.231	-0.289	-0.265
	77.5	-0.057	-0.073	-0.034	-0.095	-0.095	-0.115	-0.063	-0.182	-0.143	-0.243	-0.163	-0.293	-0.202	-0.238	-0.248	-0.300	-0.282
	83.0	-0.060	-0.077	-0.037	-0.097	-0.095	-0.115	-0.063	-0.182	-0.143	-0.243	-0.163	-0.293	-0.203	-0.238	-0.248	-0.302	-0.283
	88.7	-0.067	-0.076	-0.043	-0.100	-0.092	-0.117	-0.065	-0.183	-0.143	-0.243	-0.163	-0.293	-0.203	-0.238	-0.248	-0.303	-0.283
0.5555	0	-1.63	-1.82	-1.50	-0.83	-0.96	-0.19	-0.86	-0.93	-0.61	-0.62	-0.68	-1.19	-1.30	-1.84	-1.73	-1.92	-1.92
	1.5	-0.041	-0.093	-0.045	-0.162	-0.098	-0.223	-0.141	-0.290	-0.187	-0.313	-0.227	-0.341	-0.254	-0.384	-0.390	-0.400	-0.390
	11.2	-0.057	-0.121	-0.054	-0.208	-0.091	-0.249	-0.112	-0.307	-0.159	-0.339	-0.231	-0.354	-0.267	-0.383	-0.395	-0.409	-0.399
	21.2	-0.060	-0.115	-0.049	-0.197	-0.083	-0.242	-0.109	-0.316	-0.167	-0.346	-0.233	-0.357	-0.269	-0.383	-0.395	-0.409	-0.399
	28.7	-0.066	-0.112	-0.040	-0.197	-0.083	-0.249	-0.106	-0.317	-0.167	-0.346	-0.233	-0.357	-0.269	-0.383	-0.395	-0.409	-0.399
	36.2	-0.067	-0.108	-0.047	-0.193	-0.086	-0.248	-0.104	-0.318	-0.167	-0.347	-0.234	-0.358	-0.270	-0.384	-0.396	-0.410	-0.400
	41.7	-0.068	-0.107	-0.042	-0.191	-0.086	-0.247	-0.103	-0.317	-0.166	-0.346	-0.233	-0.357	-0.269	-0.383	-0.395	-0.409	-0.399
	53.0	-0.069	-0.108	-0.047	-0.193	-0.086	-0.248	-0.104	-0.318	-0.167	-0.347	-0.234	-0.358	-0.270	-0.384	-0.396	-0.410	-0.400
0.777	0	-1.18	-0.67	-0.67	-0.066	-0.066	-0.061	-0.167	-0.113	-0.215	-0.156	-0.159	-0.181	-0.265	-0.210	-0.301	-0.326	-0.346
	11.2	-0.092	-0.177	-0.035	-0.242	-0.043	-0.287	-0.066	-0.337	-0.139	-0.357	-0.175	-0.365	-0.217	-0.389	-0.326	-0.346	-0.365
	21.2	-0.114	-0.190	-0.043	-0.267	-0.046	-0.306	-0.054	-0.345	-0.147	-0.365	-0.203	-0.385	-0.235	-0.405	-0.346	-0.365	-0.385
	31.6	-0.117	-0.198	-0.056	-0.272	-0.046	-0.314	-0.057	-0.351	-0.151	-0.371	-0.213	-0.395	-0.243	-0.415	-0.346	-0.365	-0.385
	41.8	-0.123	-0.208	-0.053	-0.272	-0.047	-0.315	-0.058	-0.352	-0.152	-0.372	-0.214	-0.396	-0.244	-0.416	-0.347	-0.366	-0.386
	53.0	-0.125	-0.170	-0.048	-0.265	-0.047	-0.314	-										

TABLE II.- EXPERIMENTAL PRESSURE COEFFICIENTS - Continued
 $M = 1.90$

		$R = 12.6 \times 10^6$																
		$\alpha = 0^\circ$		$\alpha = 2^\circ$		$\alpha = 4^\circ$		$\alpha = 6^\circ$		$\alpha = 8^\circ$		$\alpha = 10^\circ$		$\alpha = 12^\circ$		$\alpha = 14^\circ$		
y	Sta-	c_p	c_{p_u}	c_{p_l}	c_{p_u}	c_{p_l}	c_{p_u}	c_{p_l}	c_{p_u}	c_{p_l}								
0.111	0	.215	.204	.216	.177	.196	.135	.164	.115	.122	.078	.077	.055	.050	.043	.021	.030	.061
	3.8	.042	.006	.055	.038	.118	.067	.153	.182	.194	.156	.151	.237	.279	.170	.301	.361	
	7.3	.045	-.006	.063	-.045	.096	-.062	.131	-.108	.171	-.149	.193	-.182	.250	.167	.294	-.261	
	10.8	.003	-.014	.037	-.058	.068	-.062	.108	-.103	.141	-.128	.173	-.153	.210	.123	.262	.306	
	14.2	-.004	-.039	.085	-.051	.055	-.079	.089	-.036	.126	-.119	.128	-.139	.205	.190	.279	.351	
	17.5	-.007	-.030	.083	-.050	.051	-.078	.082	-.092	.116	-.111	.146	-.113	.188	-.154	.228	-.270	
	21.2	-.012	-.074	.017	-.068	.043	-.077	.071	-.080	.108	-.111	.134	-.126	.173	-.199	.252	-.252	
	24.7	-.007	-.037	.080	-.050	.046	-.073	.076	-.088	.108	-.104	.136	-.120	.177	.118	.215	-.150	
	28.2	-.003	-.028	.080	-.050	.046	-.072	.078	-.088	.106	-.103	.136	-.118	.178	-.123	.213	-.140	
	31.7	-.019	-.030	.017	-.060	.041	-.072	.069	-.085	.102	-.103	.131	-.119	.170	-.121	.206	-.137	
	35.2	-.018	-.037	.003	-.068	.032	-.079	.060	-.091	.092	-.108	.128	-.124	.154	-.133	.195	-.115	
	38.7	-.008	-.024	.013	-.063	.026	-.086	.084	-.097	.083	-.113	.111	-.131	.151	-.143	.188	-.136	
	42.2	-.031	-.031	.003	-.065	.020	-.097	.065	-.096	.071	-.113	.103	-.127	.144	-.134	.159	-.117	
	45.7	-.003	-.028	.003	-.068	.016	-.088	.075	-.098	.073	-.113	.103	-.131	.139	-.126	.180	-.104	
	49.2	-.031	-.037	.003	-.065	.015	-.097	.066	-.098	.071	-.113	.105	-.132	.142	-.131	.160	-.120	
	52.7	-.013	-.057	.007	-.069	.015	-.092	.061	-.099	.072	-.113	.089	-.133	.137	-.119	.175	-.162	
	56.2	-.037	-.028	.013	-.073	.008	-.093	.037	-.101	.085	-.118	.093	-.135	.132	-.119	.168	-.166	
	59.7	-.043	-.036	.019	-.072	.008	-.098	.028	-.109	.057	-.115	.082	-.132	.118	-.117	.154	-.163	
	63.2	-.067	-.077	.007	-.091	.008	-.109	-.005	-.117	.032	-.130	.045	-.145	.078	-.159	.113	-.175	
0.333	0	.173	.132	.186	.069	.171	0	.140	.068	.098	.103	.068	-.146	.033	-.173	-.003	.035	
	4.8	.038	-.051	.081	-.113	.113	-.186	.156	-.256	.196	-.296	.221	-.341	.304	-.381	.334		
	8.3	-.087	-.073	.021	-.111	.086	-.209	.107	-.278	.150	-.312	.159	-.348	.247	-.312	.318		
	11.8	-.036	-.075	.007	-.117	.049	-.163	.163	-.267	.129	-.313	.169	-.349	.213	-.315	.328		
	15.3	-.034	-.076	0	-.111	.031	-.143	.073	-.200	.114	-.244	.150	-.304	.211	-.325	.328		
	18.8	-.050	-.071	-.006	-.103	.089	-.131	.066	-.205	.103	-.213	.142	-.293	.225	-.328	.265		
	22.3	-.037	-.066	-.004	-.095	.023	-.121	.068	-.168	.100	-.209	.126	-.297	.176	-.322	.219		
	25.8	-.048	-.058	-.012	-.094	.018	-.120	.053	-.152	.066	-.217	.116	-.297	.171	-.347	.216		
	29.3	-.018	-.072	.020	-.097	.020	-.117	.041	-.134	.076	-.219	.108	-.299	.146	-.329	.236		
	32.8	-.052	-.073	.026	-.094	.002	-.109	.034	-.126	.069	-.133	.100	-.208	.135	-.341	.219		
	36.3	-.048	-.071	.023	-.094	.006	-.112	.036	-.129	.066	-.129	.108	-.197	.136	-.348	.212		
	40.2	-.052	-.076	-.027	-.095	-.003	-.111	.024	-.127	.057	-.135	.097	-.210	.122	-.272	.183		
	43.7	-.049	-.069	-.024	-.091	-.003	-.109	.020	-.121	.058	-.132	.096	-.215	.123	-.298	.171		
	47.2	-.055	-.075	-.034	-.095	-.006	-.111	.023	-.128	.053	-.132	.095	-.216	.123	-.295	.175		
	50.7	-.053	-.075	-.034	-.095	-.006	-.111	.023	-.128	.053	-.132	.095	-.216	.123	-.295	.175		
	54.2	-.063	-.075	-.034	-.095	-.006	-.111	.023	-.128	.053	-.132	.095	-.216	.123	-.295	.175		
0.555	0	.167	.146	.186	.083	.094	.104	.110	-.223	.115	.074	.189	-.065	.126	-.131	-.156	-.197	
	7.5	-.065	-.077	.084	-.194	.100	-.223	.115	.256	.196	-.327	.257	-.340	.292	-.348	.320		
	11.2	-.058	-.123	.002	-.109	.056	-.259	.120	.311	.158	-.335	.195	-.348	.267	-.318	.301		
	14.8	-.066	-.114	-.025	-.109	-.008	-.272	.078	.321	.117	-.338	.157	-.343	.246	-.338	.278		
	18.4	-.061	-.118	-.019	-.108	.021	-.282	.063	.296	.104	-.308	.136	-.317	.173	-.321	.242		
	22.0	-.066	-.101	-.030	-.114	.007	-.207	.048	.246	.089	-.268	.127	-.313	.163	-.328	.252		
	25.6	-.066	-.101	-.030	-.114	.007	-.207	.048	.246	.089	-.268	.127	-.313	.163	-.328	.252		
	29.2	-.069	-.101	-.038	-.115	.006	-.200	.049	.248	.081	-.266	.128	-.317	.164	-.327	.252		
	32.8	-.066	-.098	-.037	-.131	-.003	-.183	.030	.203	.065	-.239	.102	-.305	.140	-.335	.216		
	36.3	-.066	-.098	-.037	-.131	-.003	-.183	.030	.203	.065	-.239	.102	-.305	.140	-.335	.216		
	40.2	-.066	-.098	-.037	-.131	-.003	-.183	.030	.203	.065	-.239	.102	-.305	.140	-.335	.216		
	43.7	-.075	-.099	-.046	-.125	-.018	-.166	.010	.253	.084	-.305	.079	-.331	.113	-.340	.191		
	47.2	-.068	-.106	-.060	-.126	-.018	-.166	-.003	.214	.061	-.306	.063	-.331	.095	-.347	.172		
0.777	0	.166	.074	.075	-.003	-.003	-.029	-.061	-.114	-.072	-.258	-.252	-.185	-.200	-.209	-.226	-.227	
	11.2	-.090	-.172	-.013	-.056	-.065	-.283	.099	.346	.162	-.368	.172	-.347	.210	-.344	.239	-.265	
	22.4	-.111	-.168	-.039	-.269	-.016	-.305	.055	.339	.108	-.367	.243	-.347	.188	-.340	.224	-.267	
	33.6	-.119	-.161	-.053	-.273	-.004	-.305	.049	.340	.095	-.367	.243	-.347	.188	-.340	.224	-.267	
	44.8	-.120	-.161	-.053	-.273	-.019	-.308	.023	.338	.085	-.357	.241	-.347	.184	-.340	.224	-.267	
	56.0	-.119	-.168	-.053	-.269	-.011	-.311	.019	.336	.088	-.353	.241	-.347	.186	-.340	.224	-.267	
	67.2	-.102	-.149	-.055	-.221	-.016	-.273	.023	.321	.061	-.346	.091	-.345	.134	-.327	.174	-.338	
	78.4	-.104	-.146	-.055	-.221	-.016	-.273	-.003	.214	.061	-.346	.091	-.347	.134	-.355	.174	-.345	

CONFIDENTIAL

TABLE III. - EXPERIMENTAL PRESSURE COEFFICIENTS - Continued
M = 1.93

Station		$\alpha = 0^\circ$		$\alpha = 2^\circ$		$\alpha = 4^\circ$		$\alpha = 6^\circ$		$\alpha = 8^\circ$		$\alpha = 10^\circ$		
$\frac{y}{b/2}$	Per-cent c	c_p	c_{p_u}	c_{p_l}	c_{p_u}	c_{p_l}								
0.111	0	0.193	0.182	0.194	0.159	0.175	0.129	0.151	0.094	0.069	0.068	0.075		
	3.8	.054	.020	.095	-.019	.133	-.057	.167	-.103	.195	-.155	.224		
	7.3	.017	.008	.070	-.025	.104	-.053	.137	-.089	.178	-.117	.219		
	10.6	.010	-.015	.040	-.038	.072	-.062	.105	-.090	.146	-.113	.184		
	14.2	.006	-.020	.034	-.011	.064	-.062	.100	-.086	.138	-.105	.176		
	17.5	-.004	-.019	.029	-.010	.058	-.059	.089	-.082	.124	-.102	.159		
	21.2	-.002	-.023	.022	-.013	.048	-.063	.077	-.083	.108	-.101	.143		
	24.7	-.001	-.024	.024	-.013	.049	-.061	.077	-.081	.108	-.100	.142		
	28.2	-.004	-.025	.020	-.014	.049	-.062	.072	-.082	.104	-.100	.138		
	31.7	-.007	-.027	.018	-.017	.040	-.064	.068	-.086	.100	-.101	.138		
	38.2	-.017	-.036	.018	-.057	.040	-.082	.056	-.091	.088	-.108	.135		
	43.7	-.023	-.043	.002	-.063	.021	-.076	.047	-.097	.077	-.113	.109		
	49.2	-.026	-.045	.003	-.065	.019	-.080	.044	-.097	.074	-.113	.106		
	55.0	-.036	-.055	.014	-.075	.006	-.089	.031	-.105	.059	-.119	.090		
	60.7	-.028	-.047	.005	-.068	.017	-.082	.043	-.098	.072	-.113	.104		
	66.2	-.033	-.053	.011	-.072	.011	-.087	.037	-.102	.066	-.116	.098		
	71.7	-.037	-.055	.016	-.072	.006	-.087	.032	-.103	.064	-.116	.096		
	77.5	-.040	-.060	.017	-.077	.004	-.092	.030	-.107	.059	-.121	.091		
	83.2	-.049	-.067	.028	-.084	-.007	-.098	.018	-.113	.043	-.126	.075		
	88.7	-.046	-.064	-.025	-.082	-.004	-.096	.022	-.111	-.049	-.125	.080		
	94.0	-.073	-.085	-.054	-.099	-.034	-.101	-.011	-.125	-.015	-.138	-.014		
0.333	0	.171	.134	.184	.072	.168	.007	.132	-.064	.088	-.098	.051		
	4.8	.017	-.046	.072	-.120	.118	-.172	.157	-.239	.197	-.285	.235		
	9.2	-.018	-.062	.026	-.124	.074	-.198	.113	-.258	.157	-.300	.198		
	14.2	-.033	-.069	.010	-.114	.048	-.163	.086	-.258	.128	-.293	.168		
	18.7	-.033	-.068	.005	-.109	.041	-.141	.076	-.197	.115	-.262	.155		
	23.2	-.032	-.063	.003	-.098	.036	-.128	.069	-.172	.106	-.236	.146		
	28.2	-.042	-.069	-.009	-.100	.022	-.126	.053	-.162	.089	-.234	.126		
	32.7	-.043	-.067	-.013	-.096	.017	-.120	.046	-.149	.081	-.225	.117		
	40.2	-.052	-.077	-.026	-.101	.001	-.122	.029	-.143	.062	-.200	.097		
	47.5	-.053	-.076	-.028	-.099	-.002	-.119	.028	-.136	.060	-.158	.093		
	55.0	-.056	-.075	-.031	-.096	-.007	-.128	.021	-.129	.053	-.131	.087		
	62.7	-.055	-.076	-.031	-.097	-.007	-.114	.019	-.131	.049	-.135	.082		
	70.2	-.056	-.075	-.032	-.096	-.009	-.118	.017	-.129	.048	-.135	.080		
	77.5	-.056	-.075	-.032	-.097	-.008	-.126	.017	-.128	.048	-.136	.079		
	85.0	-.063	-.081	-.036	-.100	-.019	-.117	.007	-.133	.039	-.142	.069		
	92.5	-.069	-.091	-.049	-.109	-.028	-.124	-.006	-.139	.023	-.150	.050		
0.555	0	.166	.148	.150	.087	.097	.023	.031	-.032	-.032	-.070	-.082		
	7.5	-.023	-.093	.045	-.165	.096	-.220	.137	-.284	.181	-.318	.216		
	14.2	-.055	-.118	.003	-.203	.049	-.255	.094	-.300	.137	-.329	.179		
	21.2	-.073	-.120	-.020	-.200	.020	-.267	.058	-.309	.099	-.319	.142		
	26.7	-.074	-.117	-.029	-.167	-.003	-.265	.046	-.310	.086	-.316	.125		
	35.2	-.076	-.112	-.038	-.153	-.002	-.211	.033	-.282	.072	-.302	.111		
	42.2	-.075	-.107	-.038	-.144	-.006	-.193	.030	-.247	.066	-.292	.104		
	55.0	-.080	-.106	-.047	-.138	-.020	-.175	.017	-.238	.051	-.287	.084		
	66.3	-.071	-.096	-.040	-.124	-.010	-.155	.020	-.234	.054	-.267	.089		
	77.5	-.073	-.098	-.046	-.123	-.033	-.147	.010	-.223	.043	-.289	.073		
	88.7	-.083	-.105	-.059	-.128	-.035	-.147	-.004	-.209	.025	-.292	.055		
0.777	0	.119	.098	.084	.017	.020	-.063	-.009	-.131	-.078	-.176	-.116		
	11.2	-.078	-.161	-.002	-.229	.053	-.273	.102	-.320	.146	-.342	.183		
	22.4	-.107	-.182	-.039	-.258	.017	-.295	.068	-.330	.114	-.329	.156		
	33.6	-.113	-.180	-.054	-.265	-.006	-.301	.038	-.333	.082	-.330	.121		
	44.8	-.118	-.181	-.067	-.266	-.023	-.305	.022	-.335	.064	-.330	.103		
	56.0	-.110	-.163	-.063	-.257	-.022	-.303	.019	-.334	.058	-.330	.096		
	67.2	-.106	-.150	-.063	-.228	-.023	-.300	.011	-.332	.055	-.327	.088		
	78.4	-.105	-.146	-.066	-.199	-.033	-.284	.007	-.318	.033	-.324	.078		

CONFIDENTIAL

NACA RM L53108

TABLE II. - EXPERIMENTAL PRESSURE COEFFICIENTS - Concluded
 $M = 1.93$

$R = 2.2 \times 10^6$													
Station		$\alpha = 0^\circ$		$\alpha = 2^\circ$		$\alpha = 4^\circ$		$\alpha = 6^\circ$		$\alpha = 8^\circ$		$\alpha = 10^\circ$	
$\frac{y}{b/2}$	Per-cent c	C_p	C_{p_u}	C_{p_l}									
0.111	0	0.196	0.187	0.195	0.155	0.177	0.123	0.152	0.088	0.117	0.063	0.078	
	3.8	.056	.021	.089	-.021	.125	-.056	.157	-.099	.190	-.113	.224	
	7.3	.029	.001	.060	-.029	.093	-.058	.127	-.097	.165	-.141	.204	
	10.6	.010	-.014	.037	-.040	.073	-.065	.107	-.099	.144	-.120	.184	
	14.2	.004	-.018	.031	-.042	.062	-.067	.096	-.092	.132	-.095	.168	
	17.5	.003	-.020	.029	-.043	.058	-.068	.087	-.079	.121	-.091	.157	
	21.2	0	-.022	.025	-.045	.051	-.064	.078	-.074	.110	-.091	.144	
	24.7	.001	-.021	.025	-.043	.051	-.056	.078	-.073	.110	-.089	.143	
	28.2	-.001	-.021	.021	-.042	.047	-.056	.073	-.074	.105	-.090	.138	
	31.7	-.002	-.022	.020	-.042	.045	-.057	.071	-.076	.102	-.092	.135	
	38.2	-.012	-.033	.008	-.051	.033	-.066	.059	-.084	.089	-.099	.122	
	43.7	-.017	-.037	.002	-.056	.028	-.070	.052	-.088	.082	-.104	.114	
	49.2	-.020	-.038	0	-.057	.025	-.073	.049	-.091	.078	-.107	.111	
	55.0	-.026	-.016	-.007	-.063	.016	-.078	.041	-.095	.069	-.110	.102	
	60.7	-.022	-.013	-.004	-.061	.020	-.075	.045	-.093	.074	-.108	.107	
	66.2	-.026	-.015	-.006	-.064	.016	-.078	.041	-.097	.070	-.111	.103	
	71.7	-.032	-.052	-.011	-.069	.011	-.081	.035	-.101	.064	-.115	.096	
	77.5	-.034	-.052	-.013	-.070	.009	-.086	.034	-.102	.062	-.118	.094	
	83.2	-.038	-.059	-.021	-.075	.002	-.091	.025	-.107	.053	-.122	.085	
	88.7	-.039	-.058	-.019	-.075	.004	-.092	.026	-.108	.055	-.122	.086	
	94.0	-.064	-.078	-.018	-.092	-.027	-.104	-.005	-.120	.021	-.133	.051	
0.333	0	.159	.125	.166	.065	.152	.001	.121	-.068	.075	-.105	.043	
	4.8	-.014	-.041	.064	-.106	.108	-.166	.118	-.205	.187	-.247	.224	
	9.2	-.011	-.061	.027	-.110	.066	-.150	.109	-.198	.151	-.243	.192	
	14.2	-.029	-.067	.010	-.105	.046	-.155	.084	-.210	.125	-.251	.167	
	18.7	-.030	-.064	.005	-.100	.038	-.170	.074	-.221	.113	-.254	.154	
	23.2	-.032	-.064	.002	-.106	.029	-.166	.064	-.219	.102	-.255	.136	
	28.2	-.036	-.065	.007	-.105	.022	-.151	.056	-.206	.091	-.252	.130	
	32.7	-.039	-.066	.010	-.102	.016	-.110	.048	-.175	.085	-.240	.120	
	40.2	-.047	-.071	.020	-.091	.009	-.103	.038	-.136	.068	-.218	.102	
	47.5	-.015	-.072	-.018	-.085	.005	-.105	.034	-.125	.065	-.181	.100	
	55.0	-.015	-.071	-.021	-.086	0	-.106	.028	-.123	.060	-.147	.093	
	62.7	-.017	-.066	-.023	-.087	-.002	-.104	.024	-.121	.056	-.130	.088	
	70.2	-.019	-.066	-.025	-.087	-.004	-.104	.018	-.122	.052	-.130	.084	
	77.5	-.019	-.067	-.025	-.087	-.006	-.105	.021	-.121	.050	-.130	.082	
	85.0	-.056	-.073	-.034	-.092	-.012	-.109	.017	-.125	.043	-.135	.073	
	92.5	-.060	-.077	-.037	-.098	-.013	-.113	.007	-.130	.033	-.140	.064	
0.555	0	.161	.141	.140	.085	.087	.018	.026	-.038	.051	-.077	.086	
	7.5	-.021	-.089	.041	-.159	.088	-.215	.132	-.271	.172	-.279	.212	
	14.2	-.054	-.115	-.001	-.171	.044	-.210	.089	-.258	.134	-.278	.179	
	21.2	-.069	-.120	-.025	-.165	.016	-.212	.061	-.260	.102	-.280	.145	
	28.7	-.070	-.111	-.028	-.171	.008	-.220	.056	-.266	.088	-.285	.128	
	35.2	-.070	-.107	-.017	-.172	.002	-.232	.038	-.271	.076	-.287	.116	
	42.2	-.073	-.112	-.038	-.172	-.006	-.231	.030	-.273	.067	-.290	.112	
	55.0	-.075	-.108	-.041	-.138	-.015	-.206	.018	-.271	.056	-.288	.091	
	66.3	-.070	-.100	-.034	-.104	-.003	-.149	.026	-.248	.058	-.282	.091	
	77.5	-.067	-.092	-.038	-.109	-.015	-.128	.013	-.229	.044	-.283	.083	
	88.7	-.075	-.096	-.052	-.117	-.026	-.132	0	-.208	.027	-.285	.060	
0.777	0	.126	.095	.094	.019	.029	-.063	-.027	-.134	-.079	-.180	-.118	
	11.2	-.078	.159	-.006	-.226	.053	-.271	.100	-.290	.144	-.297	.185	
	22.4	-.107	-.178	-.041	-.237	.016	-.260	.063	-.284	.110	-.297	.154	
	33.6	-.114	-.171	-.056	-.233	-.005	-.262	.038	-.236	.083	-.299	.124	
	44.8	-.116	-.168	-.069	-.239	-.021	-.267	.019	-.268	.061	-.302	.101	
	56.0	-.110	-.168	-.067	-.242	-.025	-.272	.014	-.289	.053	-.304	.093	
	67.2	-.104	-.166	-.063	-.239	-.024	-.279	.012	-.291	.053	-.305	.098	
	78.4	-.106	-.164	-.069	-.238	-.032	-.275	.012	-.291	.043	-.306	.092	

CONFIDENTIAL

TABLE III. - EXPERIMENTAL PRESSURE COEFFICIENTS

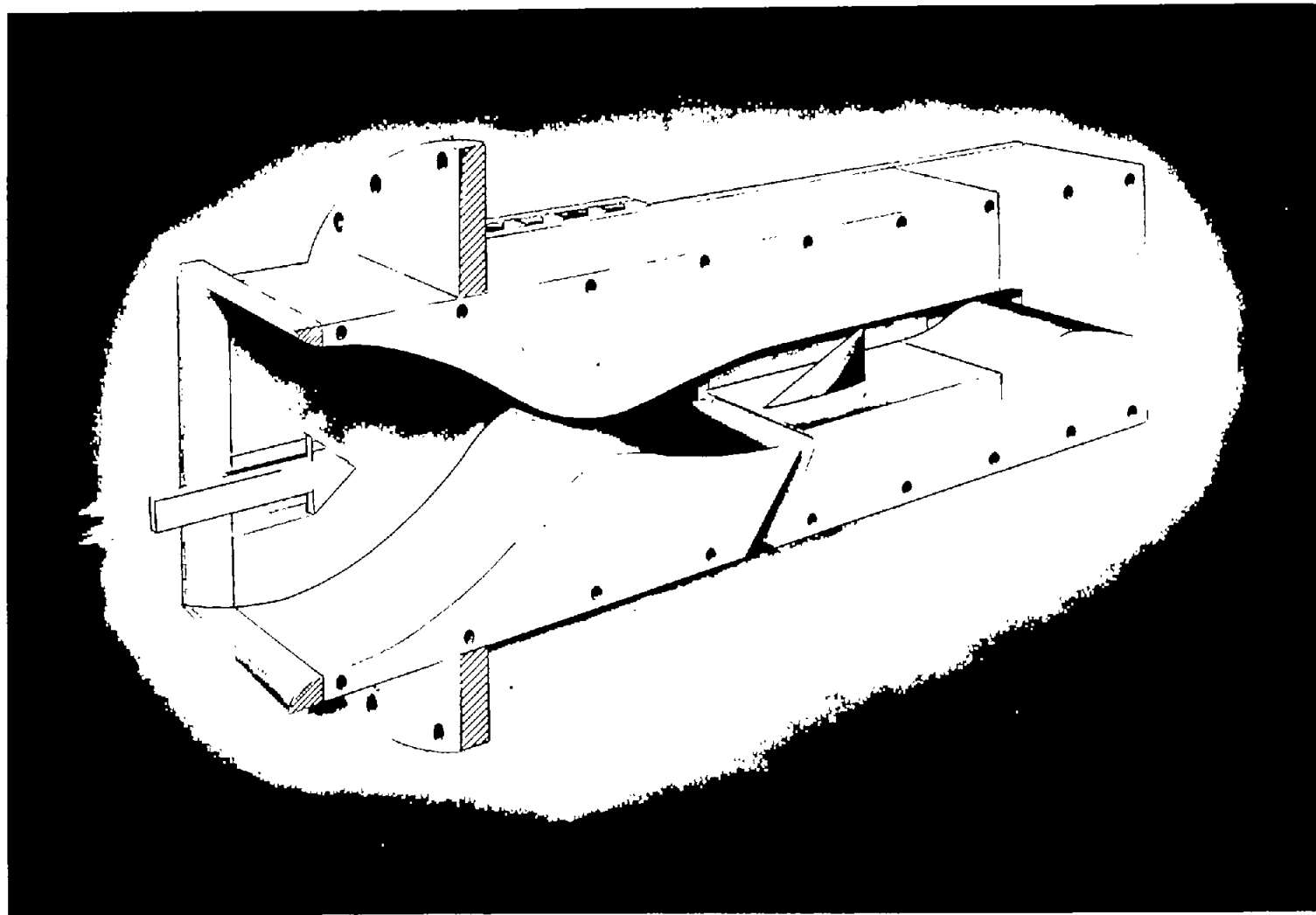
 $M = 1.62$

Station		$\alpha = 0^\circ$		$\alpha = 2^\circ$		$\alpha = 4^\circ$		$\alpha = 6^\circ$		$\alpha = 8^\circ$		$\alpha = 10^\circ$	
y $b/2$	Per- cent c	c_p	c_{p_u}	c_{p_l}									
0.111	0	0.210	0.193	0.201	0.163	0.181	0.122	0.147	0.068	0.098	0.023	0.037	
	3.8	.048	.009	.094	-.029	.134	-.068	.168	-.113	.203	-.154	.239	
	7.3	.052	.018	.086	-.017	.124	-.051	.163	-.086	.205	-.122	.251	
	10.6	.030	0	.063	-.031	.096	-.060	.131	-.090	.168	-.117	.210	
	14.2	.025	-.001	.056	-.031	.088	-.060	.121	-.086	.158	-.110	.200	
	17.5	.017	-.010	.048	-.037	.079	-.062	.113	-.086	.149	-.109	.187	
	21.2	.008	-.016	.038	-.041	.067	-.064	.099	-.087	.135	-.108	.174	
	24.7	.008	-.015	.037	-.040	.066	-.061	.098	-.084	.133	-.105	.171	
	28.2	.006	-.018	.033	-.041	.062	-.062	.093	-.084	.128	-.105	.166	
	31.7	.003	-.021	.029	-.043	.057	-.063	.087	-.086	.120	-.107	.157	
	38.2	-.009	-.031	.016	-.053	.043	-.073	.072	-.094	.106	-.114	.142	
	43.7	-.014	-.036	.012	-.058	.039	-.078	.067	-.099	.100	-.118	.136	
	49.2	-.017	-.039	.008	-.060	.035	-.079	.063	-.099	.095	-.118	.129	
	55.0												
	60.7	-.021	-.042	.005	-.063	.031	-.081	.060	-.099	.093	-.116	.125	
	66.2	-.029	-.050	-.004	-.071	.024	-.089	.050	-.107	.081	-.125	.117	
	71.7	-.036	-.057	-.013	-.076	.013	-.093	.041	-.111	.072	-.128	.106	
	77.5	-.043	-.063	-.021	-.082	.004	-.099	.031	-.117	.063	-.134	.097	
	83.2	-.061	-.080	-.010	-.098	-.017	-.114	.010	-.131	.040	-.147	.073	
	88.7	-.056	-.075	-.033	-.093	-.008	-.110	.020	-.128	.053	-.143	.092	
	94.0	-.089	-.103	-.072	-.118	-.052	-.133	-.024	-.149	.008	-.163	.052	
0.333	0	.184	.135	.192	.041	.157	-.067	.100	-.152	.042	-.199	-.014	
	4.8	.021	-.035	.082	-.128	.131	-.249	.174	-.343	.214	-.418	.252	
	9.2	-.012	-.065	.011	-.131	.089	-.188	.130	-.328	.175	-.399	.219	
	14.2	-.024	-.069	.021	-.122	.065	-.165	.107	-.328	.150	-.362	.193	
	18.7	-.021	-.061	.020	-.103	.285	-.141	.099	-.223	.140	-.332	.183	
	23.2	-.020	-.056	.017	-.093	.054	-.126	.091	-.181	.130	-.277	.172	
	28.2	-.033	-.064	.001	-.097	.036	-.127	.070	-.158	.108	-.191	.149	
	32.7	-.035	-.064	-.003	-.094	.030	-.121	.065	-.156	.101	-.130	.141	
	40.2	-.047	-.074	-.017	-.101	.015	-.126	.050	-.148	.084	-.155	.123	
	47.5	-.046	-.070	-.017	-.095	.014	-.117	.043	-.151	.076	-.148	.114	
	55.0	-.048	-.071	-.021	-.096	.007	-.118	.046	-.140	.079	-.150	.116	
	62.7	-.049	-.070	-.024	-.092	.004	-.113	.034	-.134	.064	-.149	.101	
	70.2	-.054	-.076	-.030	-.098	-.003	-.117	.026	-.138	.055	-.152	.091	
	77.5	-.060	-.080	-.037	-.101	-.010	-.119	.017	-.140	.050	-.153	.084	
	85.0	-.075	-.093	-.053	-.115	-.026	-.134	-.004	-.154	.033	-.167	.067	
	92.5	-.088	-.108	-.063	-.127	-.040	-.144	-.008	-.162	.024	-.174	.070	
0.555	0	.171	.134	.144	.040	.054	-.061	-.050	-.135	-.139	-.184	-.200	
	7.5	-.014	-.105	.060	-.233	.116	-.320	.162	-.426	.202	-.435	.237	
	14.2	-.048	-.116	.015	-.211	.068	-.344	.116	-.420	.160	-.426	.202	
	21.2	-.063	-.117	-.012	-.183	.038	-.273	.083	-.394	.127	-.407	.168	
	28.7	-.065	-.108	-.020	-.160	.023	-.215	.066	-.352	.107	-.383	.148	
	35.2	-.069	-.110	-.029	-.153	.011	-.192	.051	-.342	.096	-.380	.140	
	42.2	-.071	-.106	-.032	-.145	.012	-.177	.052	-.325	.089	-.387	.127	
	55.0	-.079	-.105	-.055	-.137	-.009	-.167	.022	-.240	.061	-.404	.099	
	66.3	-.070	-.100	-.040	-.129	-.010	-.149	.021	-.134	.057	-.381	.087	
	77.5	-.086	-.113	-.057	-.139	-.029	-.159	-.005	-.158	.042	-.364	.083	
	88.7	-.102	-.129	-.073	-.153	-.039	-.174	-.009	-.180	.023	-.286	.058	
0.777	0	.132	.083	.065	-.057	-.046	-.177	-.125	-.264	-.191	-.323	-.242	
	11.2	-.103	-.219	-.001	-.345	.065	-.419	.114	-.483	.154	-.448	.191	
	22.4	-.115	-.220	-.032	-.368	.025	-.433	.073	-.467	.116	-.405	.154	
	33.6	-.119	-.197	-.058	-.353	-.008	-.434	.036	-.464	.080	-.383	.122	
	44.8	-.129	-.186	-.078	-.271	-.027	-.424	.014	-.453	.080	-.391	.098	
	56.0	-.126	-.167	-.074	-.229	-.026	-.351	.014	-.431	.080	-.397	.101	
	67.2	-.119	-.164	-.072	-.210	-.029	-.325	.015	-.425	.059	-.402	.107	
	78.4	-.125	-.165	-.083	-.206	-.039	-.324	.003	-.420	.046	-.408	.085	

TABLE III. - EXPERIMENTAL PRESSURE COEFFICIENTS - Concluded

M = 1.62

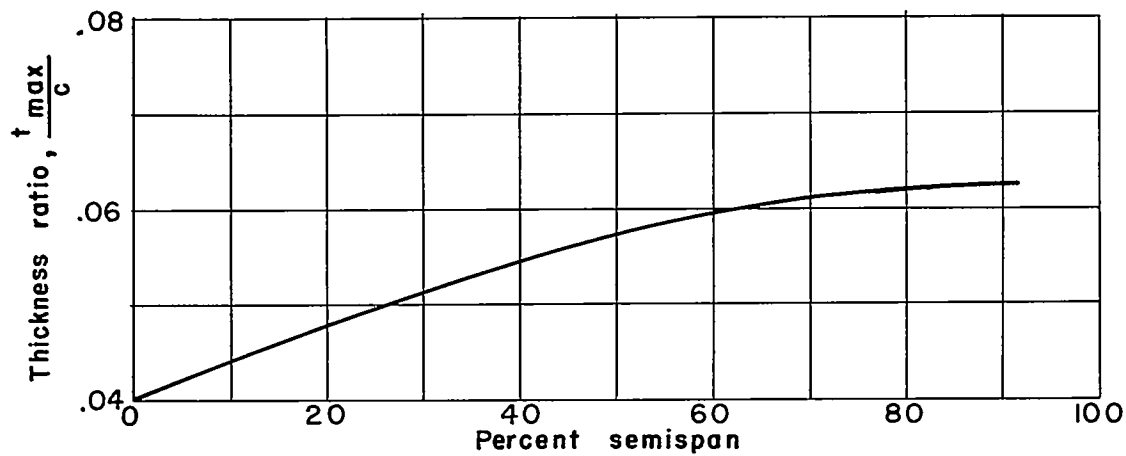
Station		$\alpha = 0^\circ$		$\alpha = 2^\circ$		$\alpha = 4^\circ$		$\alpha = 6^\circ$		$\alpha = 8^\circ$		$\alpha = 10^\circ$		
y $b/2$	Per- cent c	c_p	c_{p_u}	c_{p_l}	c_{p_u}	c_{p_l}								
0.111	0	0.201	0.187	0.190	0.156	0.172	0.116	0.137	0.068	0.091	0.020	0.036		
	3.8	.048	.009	.081	-.027	.125	-.065	.160	-.114	.196	-.178	.233		
	7.3	.035	.002	.066	-.033	.106	-.065	.145	-.110	.189	-.133	.232		
	10.6	.019	-.011	.046	-.042	.084	-.071	.119	-.100	.156	-.116	.196		
	14.2	.014	-.014	.014	-.045	.081	-.071	.114	-.089	.151	-.109	.187		
	17.5	.009	-.019	.037	-.017	.071	-.068	.103	-.084	.139	-.108	.178		
	21.2	.008	-.021	.032	-.047	.064	-.063	.095	-.083	.130	-.106	.168		
	24.7	.008	-.020	.031	-.043	.062	-.060	.092	-.080	.126	-.104	.163		
	28.2	.005	-.019	.027	-.041	.057	-.061	.086	-.080	.121	-.103	.158		
	31.7	.002	-.022	.023	-.044	.053	-.062	.083	-.084	.115	-.106	.151		
	38.2	-.008	-.030	.014	-.053	.040	-.071	.070	-.091	.102	-.113	.137		
	43.7	-.014	-.037	.008	-.058	.035	-.077	.063	-.096	.095	-.118	.130		
	49.2	-.017	-.038	.004	-.060	.032	-.078	.061	-.098	.092	-.119	.125		
	55.0													
	60.7	-.020	-.042	-.001	-.062	.027	-.082	.055	-.102	.087	-.122	.121		
	66.2	-.026	-.046	-.007	-.068	.021	-.086	.049	-.107	.081	-.126	.115		
	71.7	-.036	-.056	-.017	-.076	.011	-.094	.039	-.113	.070	-.131	.103		
	77.5	-.041	-.060	-.023	-.080	.005	-.098	.032	-.118	.064	-.137	.099		
	83.2	-.051	-.069	-.032	-.089	-.005	-.106	.023	-.125	.054	-.144	.092		
	88.7	-.051	-.071	-.031	-.090	-.005	-.109	.026	-.126	.062	-.143	.104		
	94.0	-.081	-.095	-.068	-.111	-.044	-.128	-.014	-.146	.026	-.163	.078		
0.333	0	.165	.119	.173	.032	.143	-.072	.091	-.163	.030	-.205	-.022		
	4.8	.011	-.049	.071	-.133	.118	-.195	.159	-.280	.200	-.352	.240		
	9.2	-.018	-.071	.034	-.129	.077	-.185	.121	-.295	.166	-.355	.211		
	14.2	-.029	-.074	.016	-.116	.057	-.197	.097	-.287	.143	-.349	.189		
	18.7	-.030	-.068	.012	-.119	.050	-.185	.089	-.240	.132	-.312	.174		
	23.2	-.032	-.068	.005	-.116	.040	-.138	.077	-.152	.128	-.279	.164		
	28.2	-.038	-.070	-.002	-.111	.031	-.107	.065	-.143	.106	-.250	.146		
	32.7	-.039	-.071	-.008	-.096	.023	-.108	.059	-.139	.098	-.214	.136		
	40.2	-.047	-.076	-.017	-.095	.014	-.118	.048	-.145	.083	-.171	.121		
	47.5	-.046	-.075	-.018	-.091	.016	-.114	.043	-.137	.078	-.146	.114		
	55.0	-.047	-.070	-.018	-.092	.015	-.113	.044	-.136	.078	-.147	.110		
	62.7	-.053	-.068	-.023	-.091	-.004	-.110	.032	-.135	.066	-.146	.098		
	70.2	-.056	-.071	-.026	-.095	-.005	-.114	.023	-.138	.057	-.149	.089		
	77.5	-.061	-.077	-.035	-.100	-.011	-.119	.017	-.141	.051	-.153	.086		
	85.0	-.071	-.089	-.047	-.110	-.020	-.129	.010	-.152	.044	-.164	.083		
	92.5	-.074	-.091	-.052	-.114	-.020	-.133	.014	-.155	.054	-.168	.110		
0.555	0	.161	.122	.128	.035	.044	-.061	-.054	-.140	-.142	-.189	-.202		
	7.5	-.026	-.113	.046	-.214	.101	-.300	.145	-.370	.189	-.379	.229		
	14.2	-.059	-.122	.005	-.201	.056	-.297	.102	-.382	.151	-.386	.196		
	21.2	-.070	-.122	-.018	-.203	.029	-.294	.070	-.381	.118	-.384	.164		
	28.7	-.071	-.117	-.026	-.197	.016	-.279	.057	-.371	.101	-.384	.146		
	35.2	-.073	-.115	-.032	-.182	.008	-.193	.051	-.360	.097	-.386	.140		
	42.2	-.075	-.119	-.035	-.138	.005	-.157	.041	-.274	.080	-.390	.121		
	55.0	-.081	-.115	-.047	-.126	-.020	-.152	.020	-.194	.057	-.400	.095		
	66.3	-.080	-.099	-.046	-.125	-.009	-.149	.023	-.175	.056	-.400	.092		
	77.5	-.090	-.105	-.055	-.134	-.022	-.156	.008	-.182	.052	-.401	.089		
	88.7	-.098	-.116	-.060	-.116	-.033	-.167	.005	-.190	.034	-.335	.077		
0.777	0	.121	.075	-.054	-.055	-.051	-.177	-.130	-.266	-.198	-.321	-.249		
	11.2	-.100	-.210	-.008	-.325	.060	-.357	.108	-.394	.152	-.403	.185		
	22.4	-.116	-.204	-.044	-.322	.017	-.367	.067	-.399	.113	-.404	.153		
	33.6	-.124	-.193	-.066	-.322	-.012	-.376	.035	-.404	.080	-.402	.123		
	44.8	-.132	-.199	-.082	-.319	-.032	-.384	.013	-.408	.059	-.406	.106		
	56.0	-.128	-.193	-.083	-.298	-.034	-.376	.010	-.411	.060	-.412	.108		
	67.2	-.123	-.178	-.078	-.247	-.029	-.355	.015	-.409	.067	-.418	.112		
	78.4	-.127	-.175	-.083	-.178	-.037	-.322	.008	-.408	.051	-.426	.089		



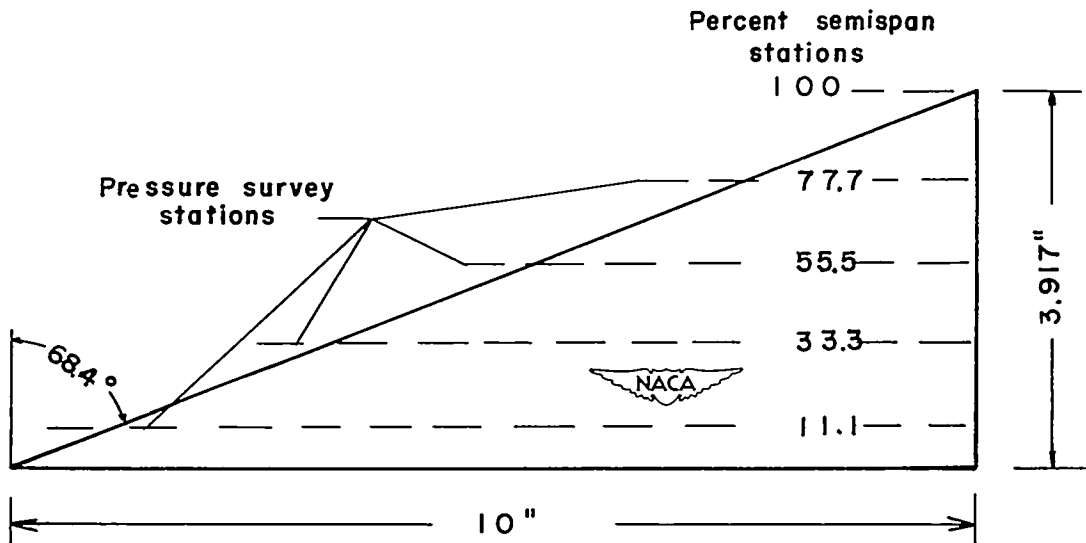
L-80472

23

Figure 1.- $M = 1.90$ blowdown jet.

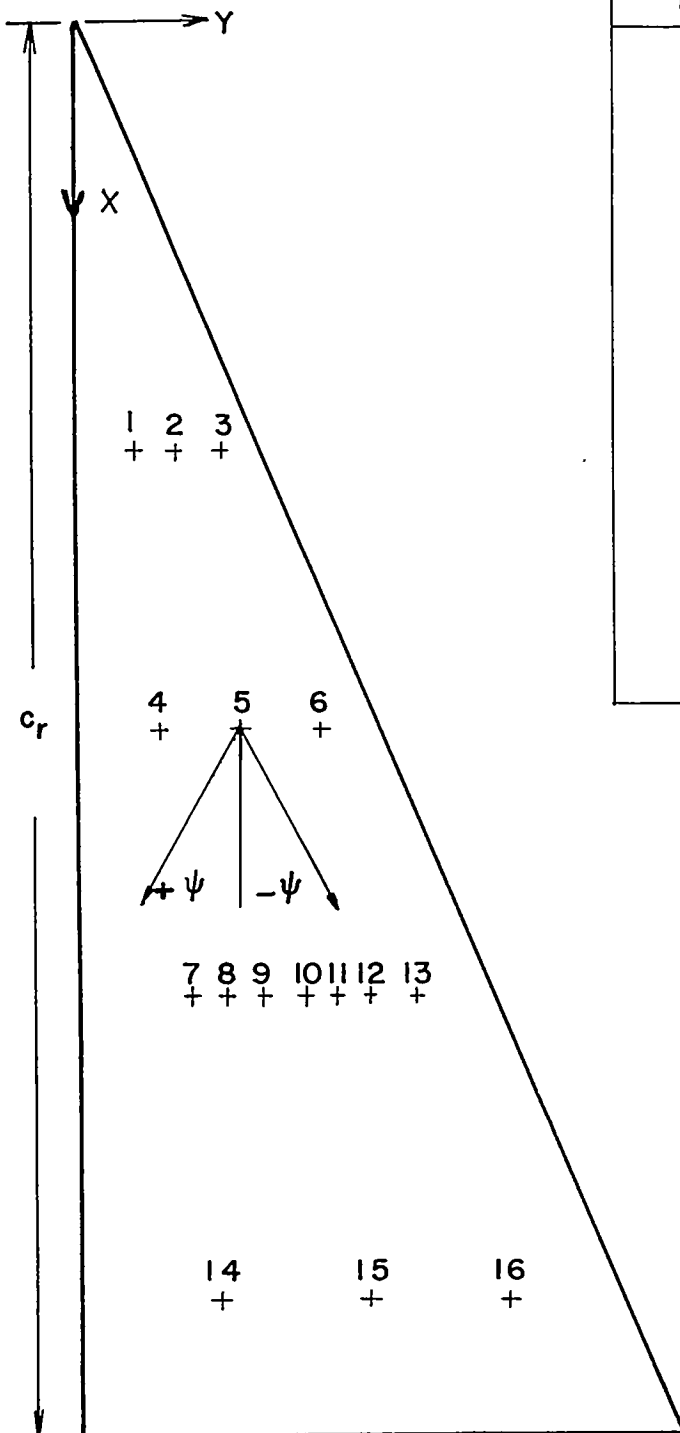


(a) Spanwise variation of maximum thickness ratio.

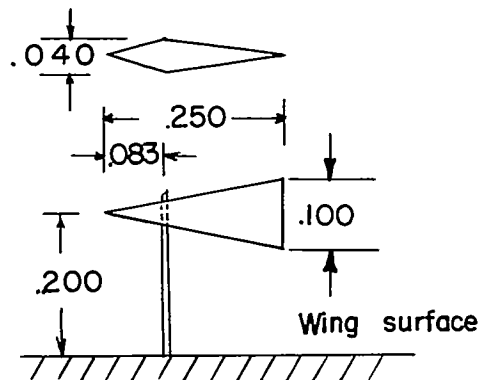


(b) Sketch of wing and pressure survey stations.

Figure 2.- Spanwise variation of maximum thickness ratio and location of pressure-survey stations.



Vane no.	Vane location	
	x/c_r	y/c_r
1	0.300	0.035
2	.300	.068
3	.300	.100
4	.500	.055
5	.500	.113
6	.500	.170
7	.700	.078
8	.700	.105
9	.700	.128
10	.700	.158
11	.700	.180
12	.700	.208
13	.700	.235
14	.900	.100
15	.900	.200
16	.900	.300



Weather cocking vane



Figure 3.- Location of flow-survey vane on wing upper surface.

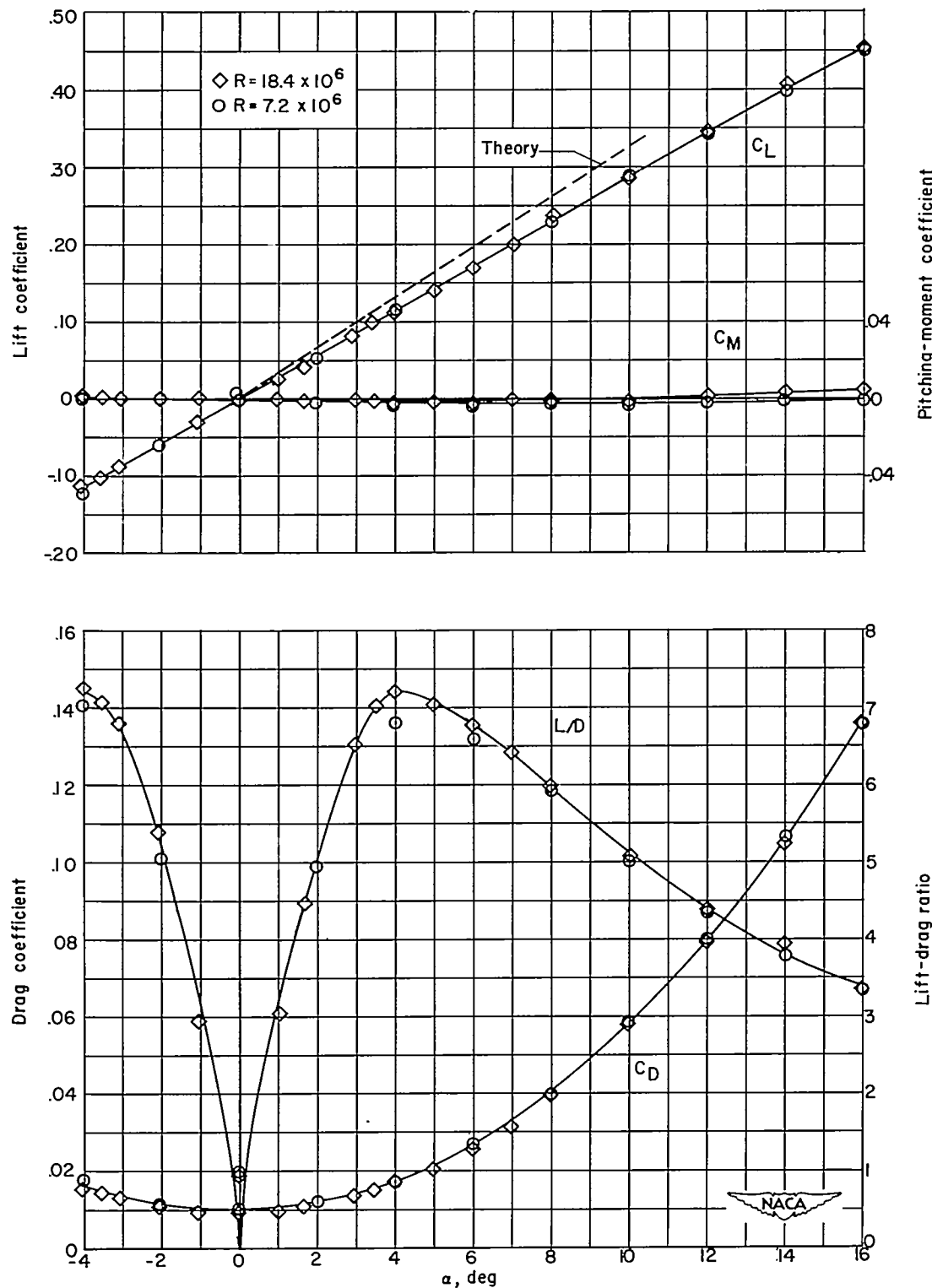


Figure 4.- Variation of wing aerodynamic characteristics with angle of attack for different Reynolds numbers. $M = 1.90$.

CONFIDENTIAL

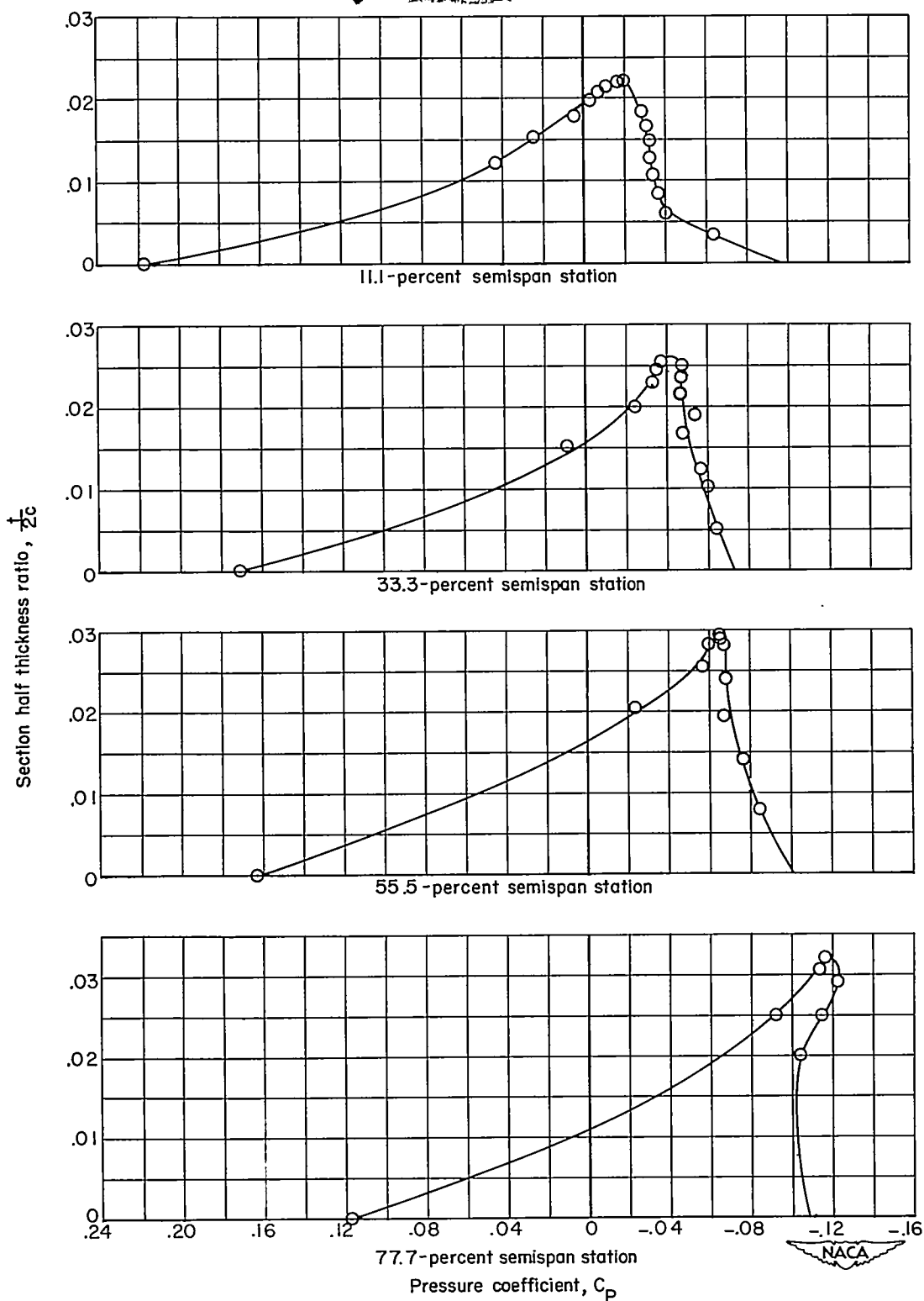


Figure 5.- Variation of pressure coefficient with thickness ratio.
 $M = 1.90$; $R = 18.4 \times 10^6$; $\alpha = 0^\circ$.

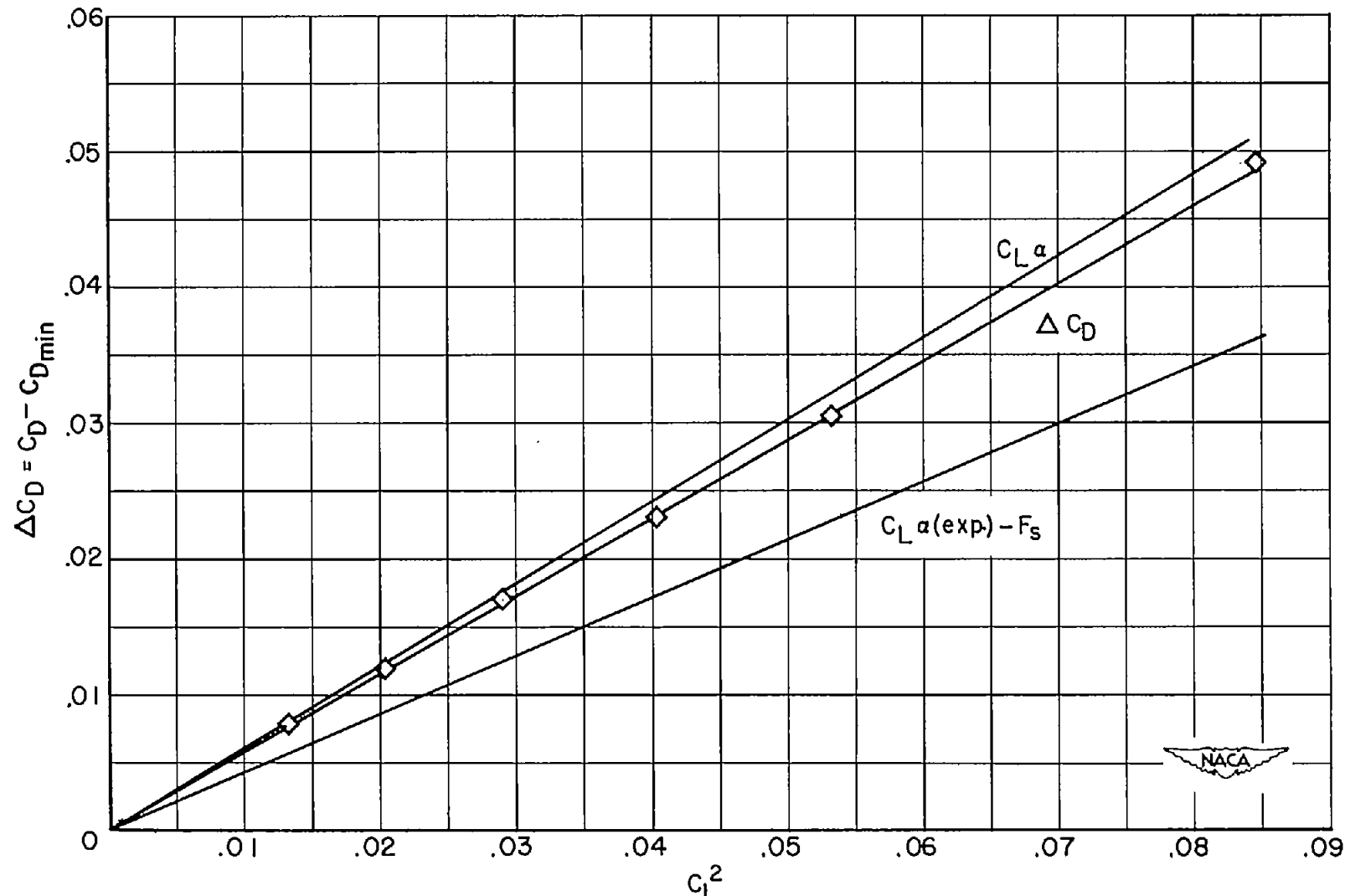


Figure 6.- Variation of ΔC_D with C_L^2 . $M = 1.90$; $R = 18.4 \times 10^6$.

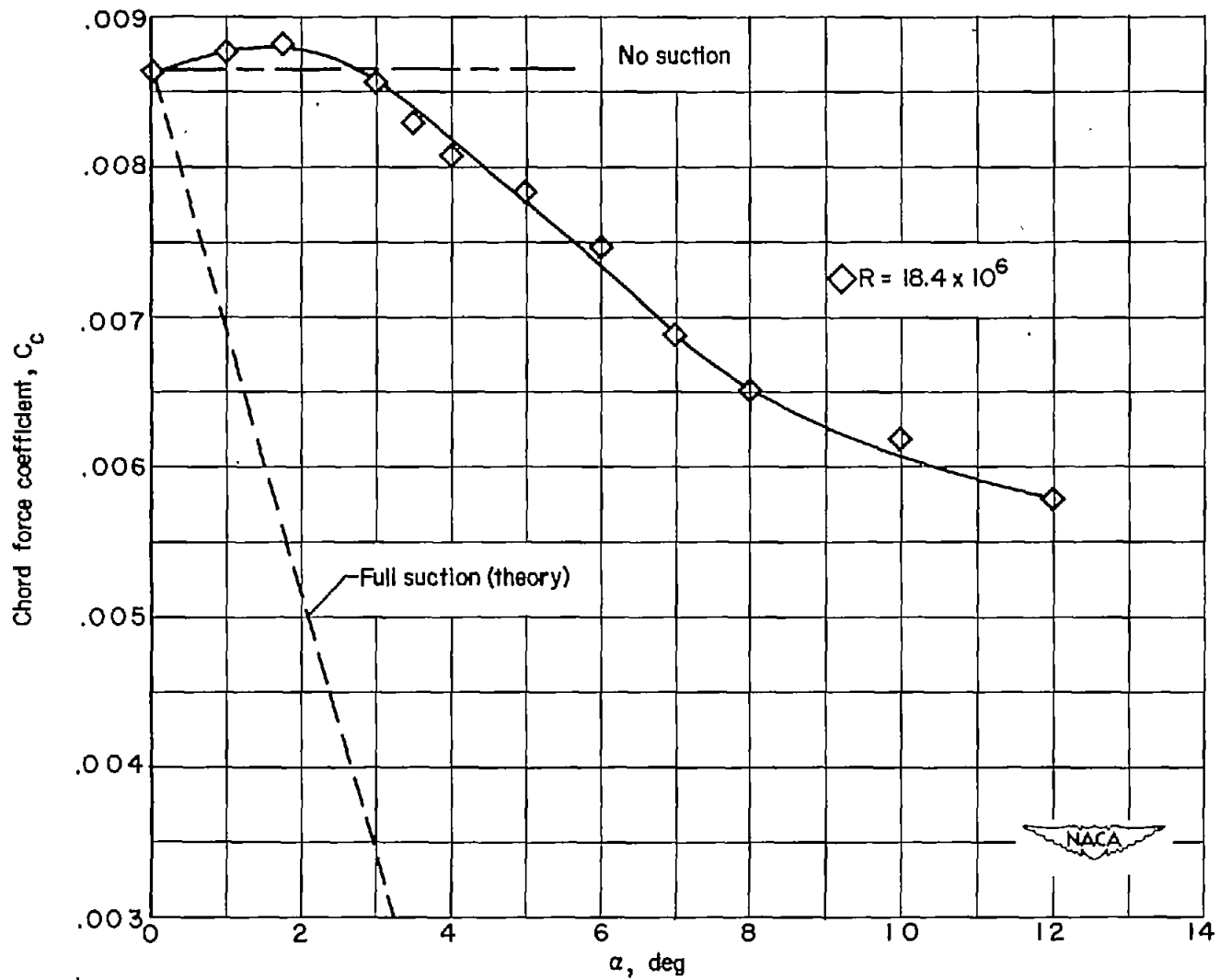


Figure 7.- Comparison of experimental and theoretical chord-force coefficients. $M = 1.90$.

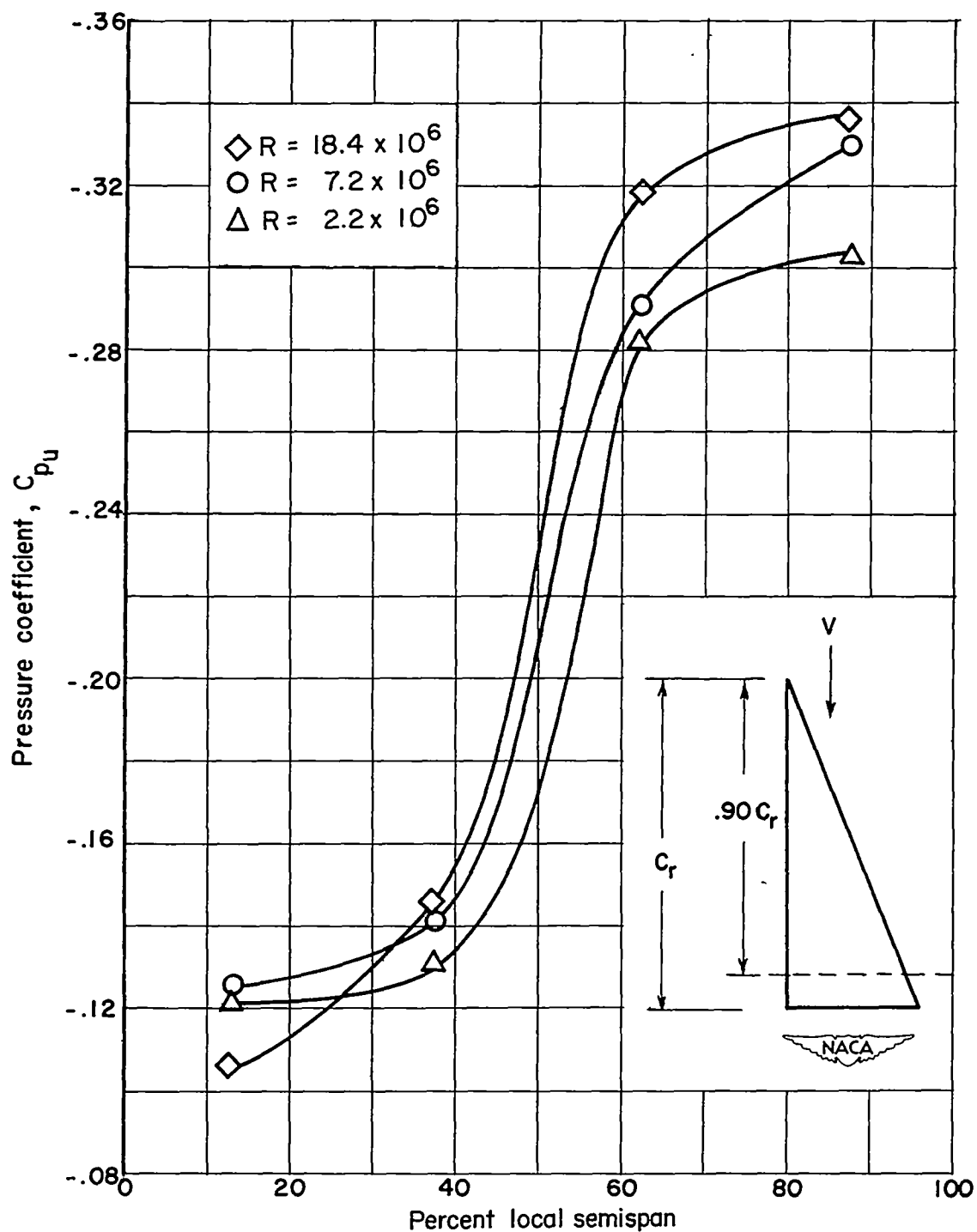


Figure 8.- Spanwise variation of upper-surface pressure coefficient at $0.90C_r$ at different Reynolds numbers. $M = 1.90$; $\alpha = 10^\circ$.

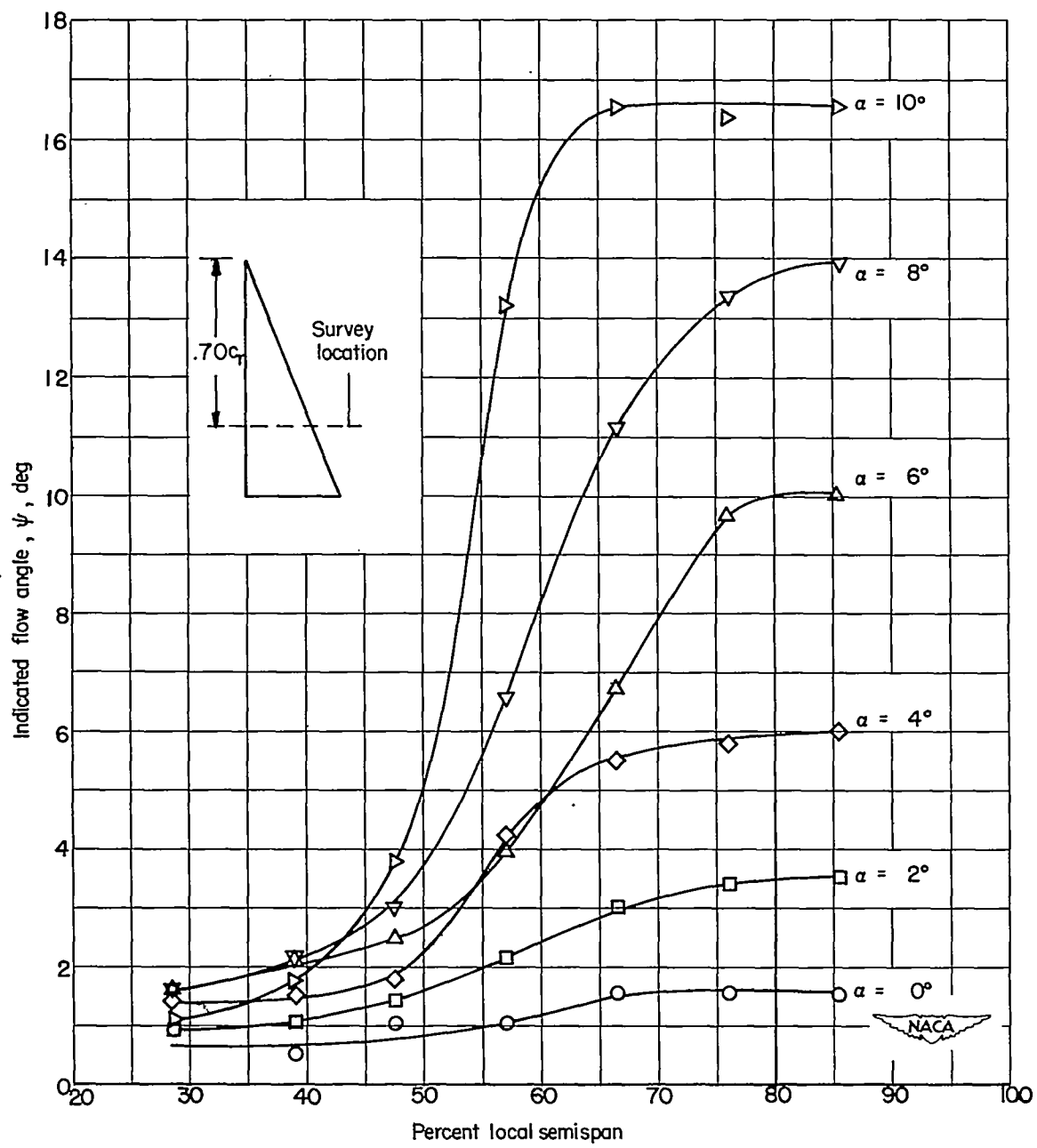
(a) $M = 1.93$.

Figure 9.- Measured local flow angles at $0.70c_r$ station. $R = 1.3 \times 10^6$.

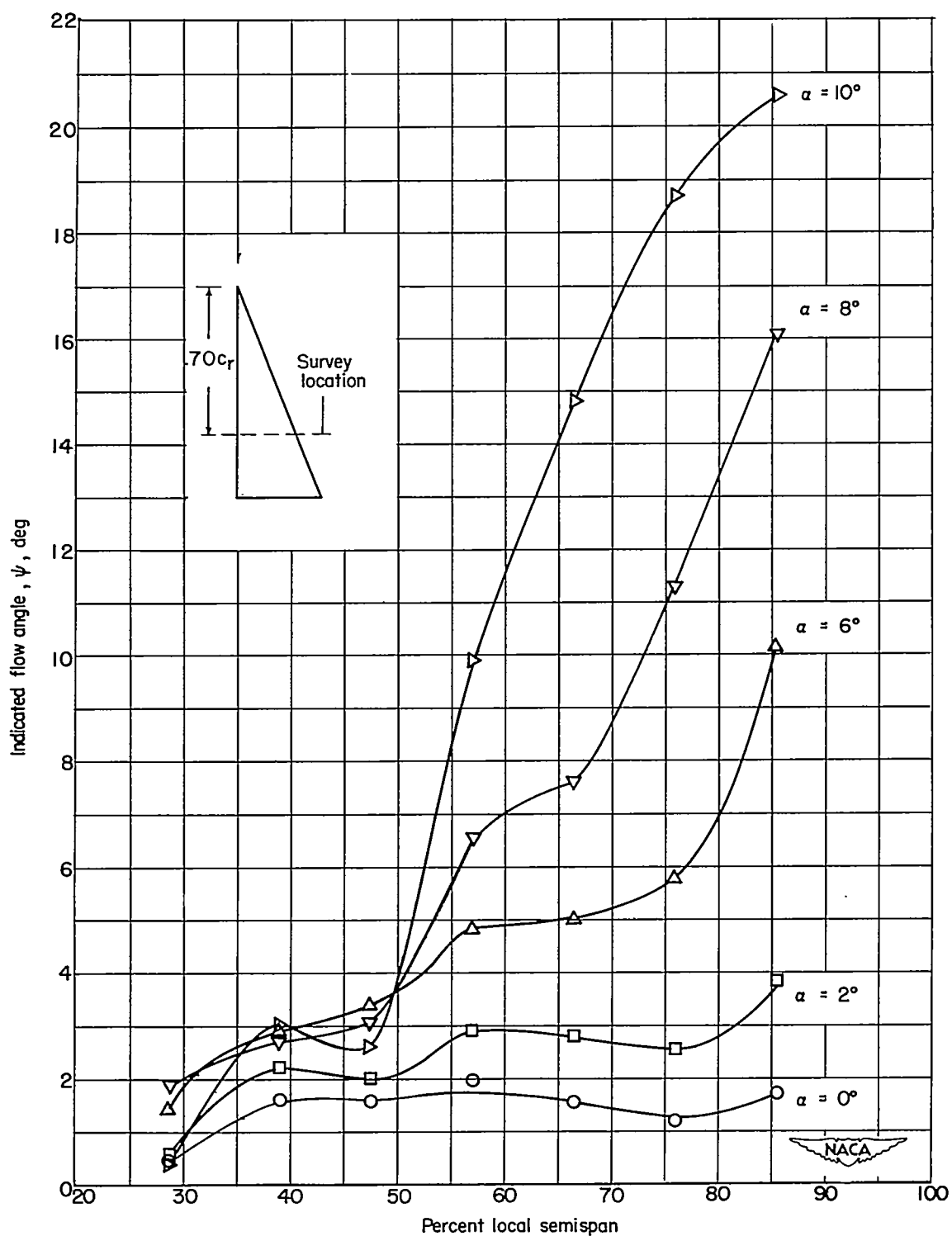
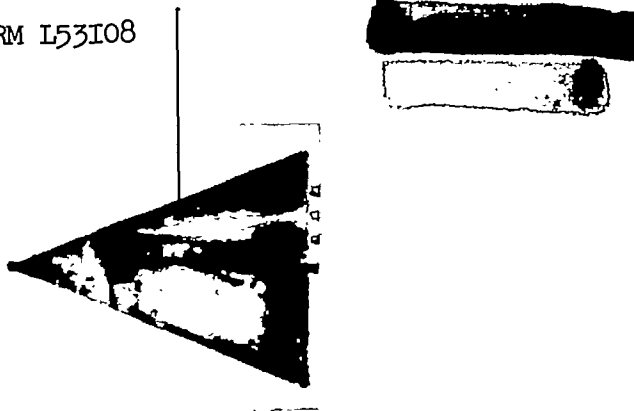
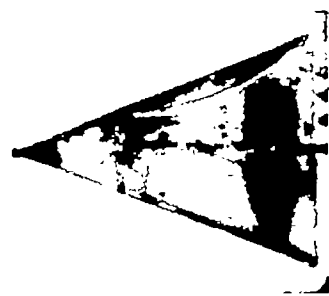
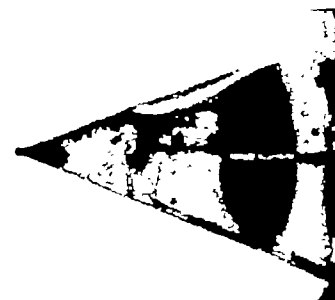
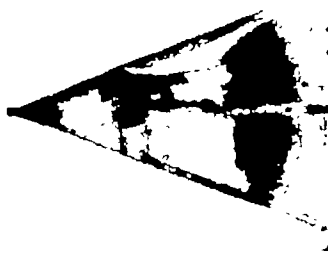
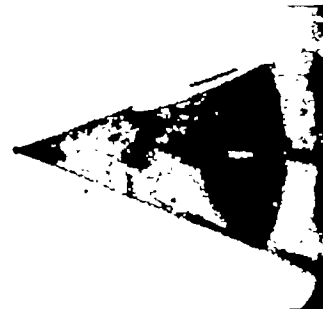
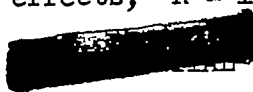
(b) $M = 1.62$.

Figure 9.- Concluded.

 $\alpha = 0^\circ$  $\alpha = 2^\circ$ $\alpha = 6^\circ$  $\alpha = 4^\circ$ $\alpha = 8^\circ$ 

L-81213

Figure 10.- Ink-flow studies of boundary-layer flow on wing upper surface.
Angle-of-attack effects; $R = 1.3 \times 10^6$; $M = 1.93$.

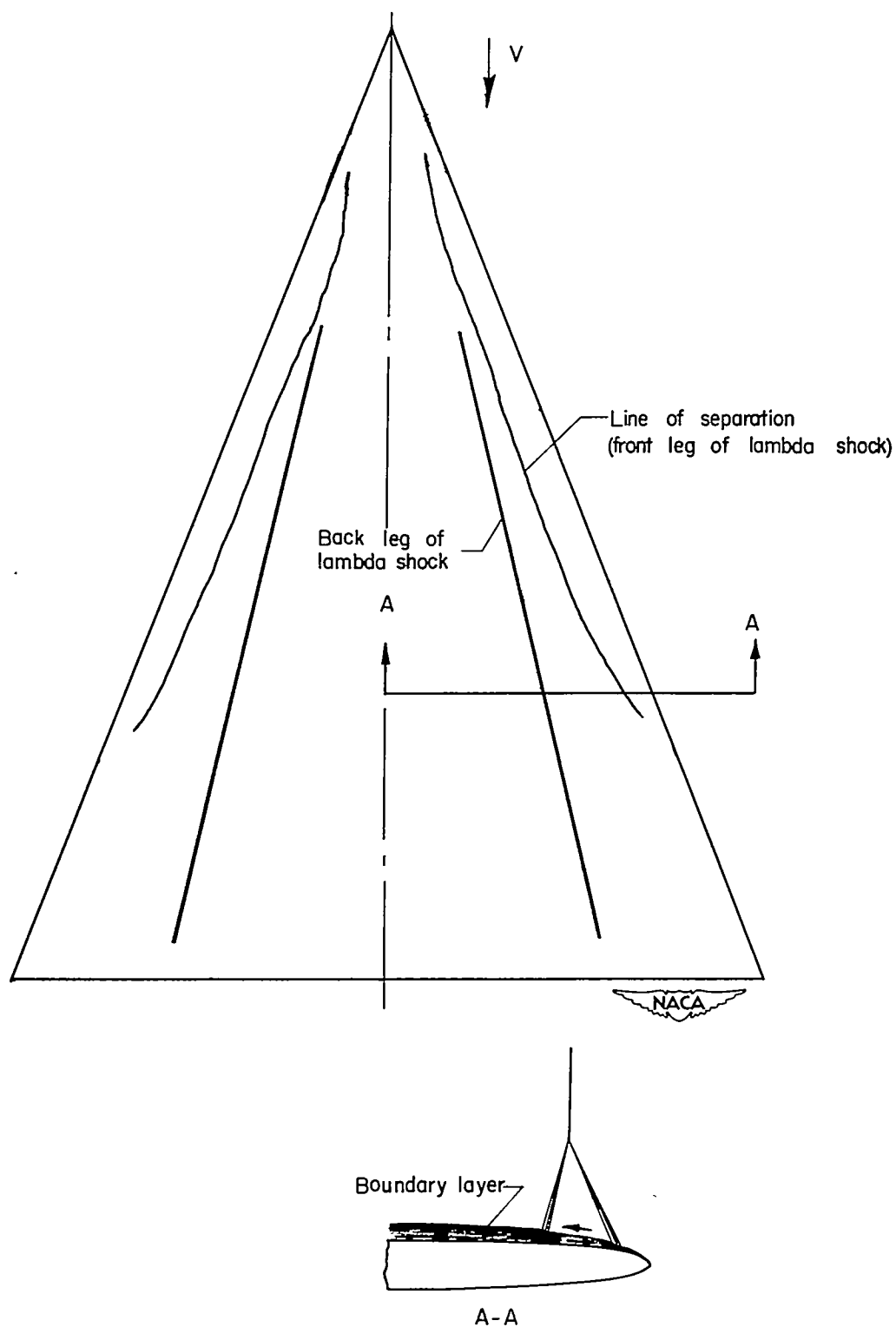
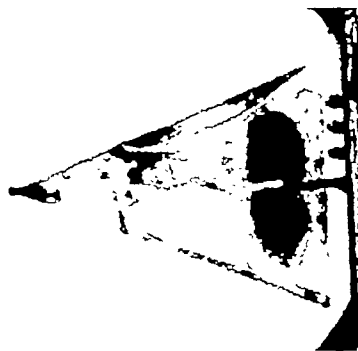
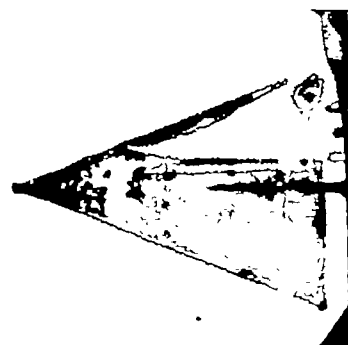


Figure 11.-- Pictorial sketch of flow over the wing upper surface at moderate angles of attack. $M = 1.90$.

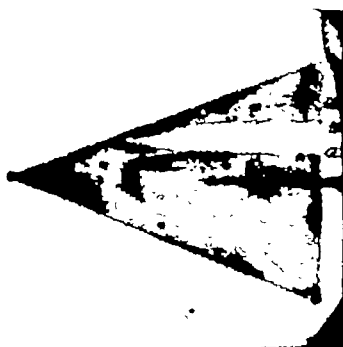
C



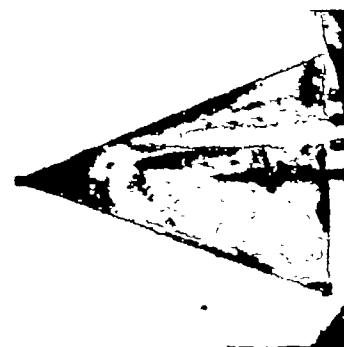
$$R = 1 \times 10^6$$



$$R = 3 \times 10^6$$



$$R = 3.5 \times 10^6$$



$$R = 5 \times 10^6$$

L-81214

Figure 12.-- Ink-flow studies of boundary-layer flow on wing upper surface.
Reynolds number effects; $\alpha = 2^\circ$; $M = 1.93$.

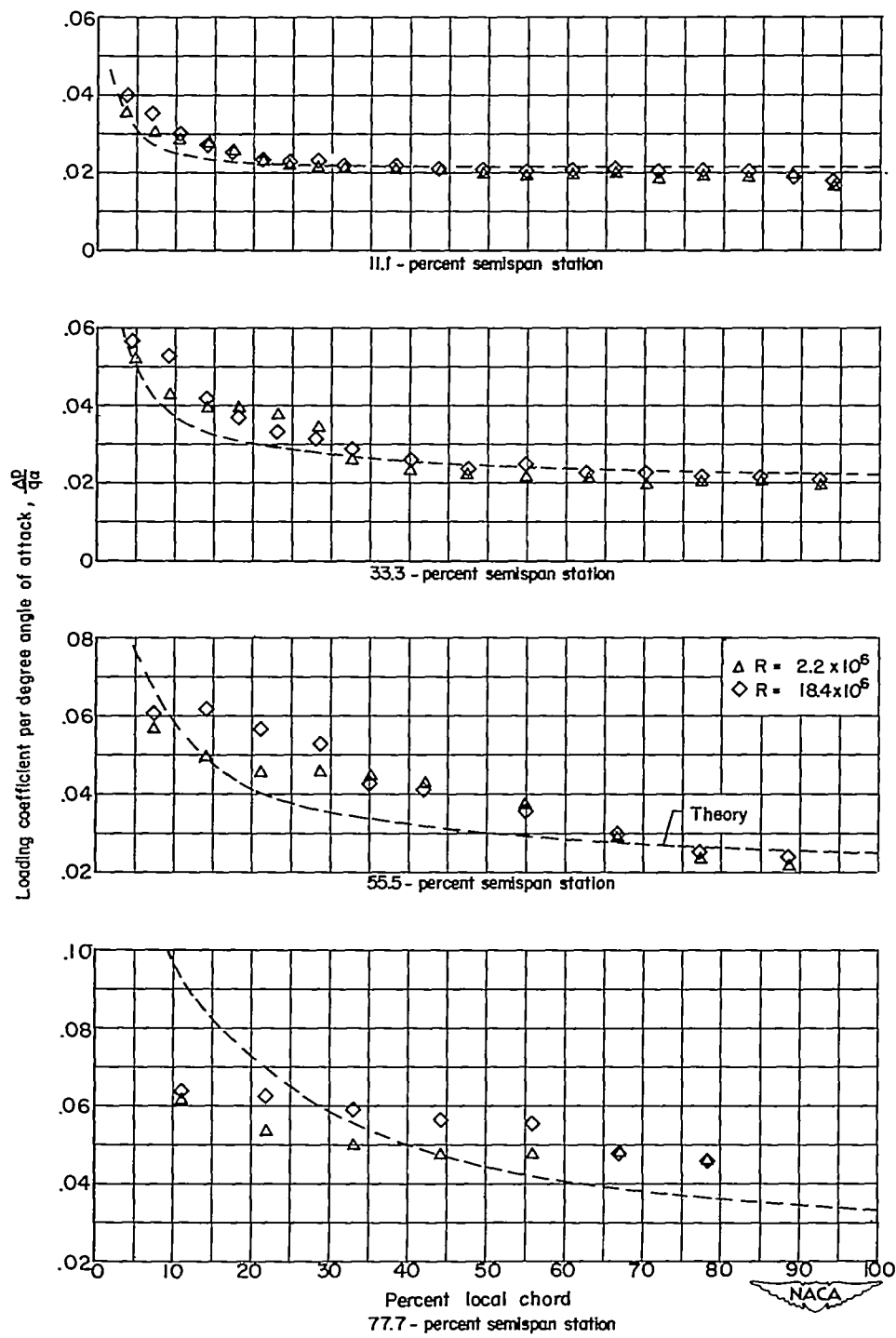
(a) $M = 1.90$.

Figure 13.- Chordwise variation of loading coefficients at different Reynolds numbers. $\alpha = 6^\circ$.

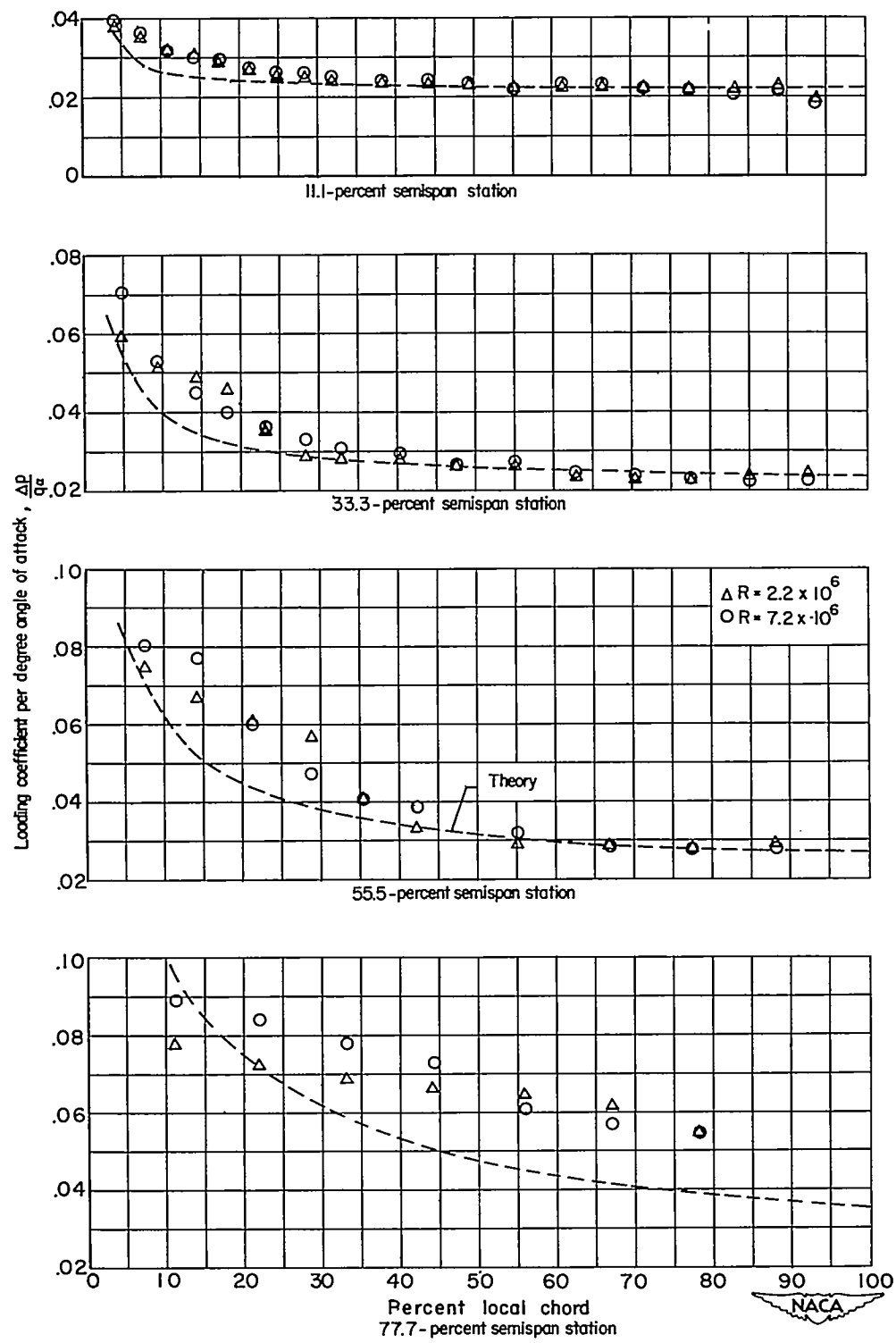
(b) $M = 1.62$.

Figure 13.- Concluded.

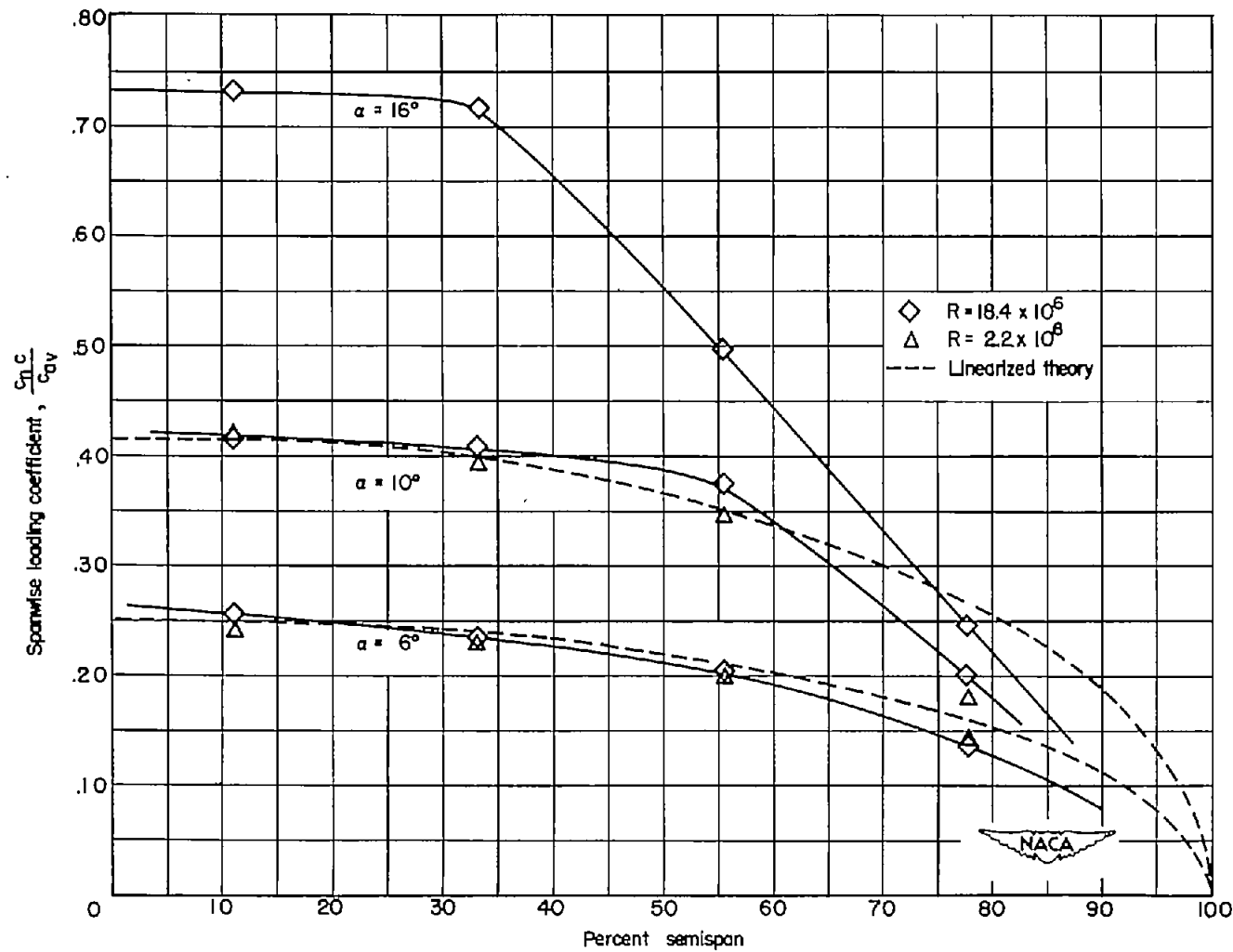
(a) $M = 1.90$.

Figure 14.- Spanwise load distribution at different Reynolds numbers.

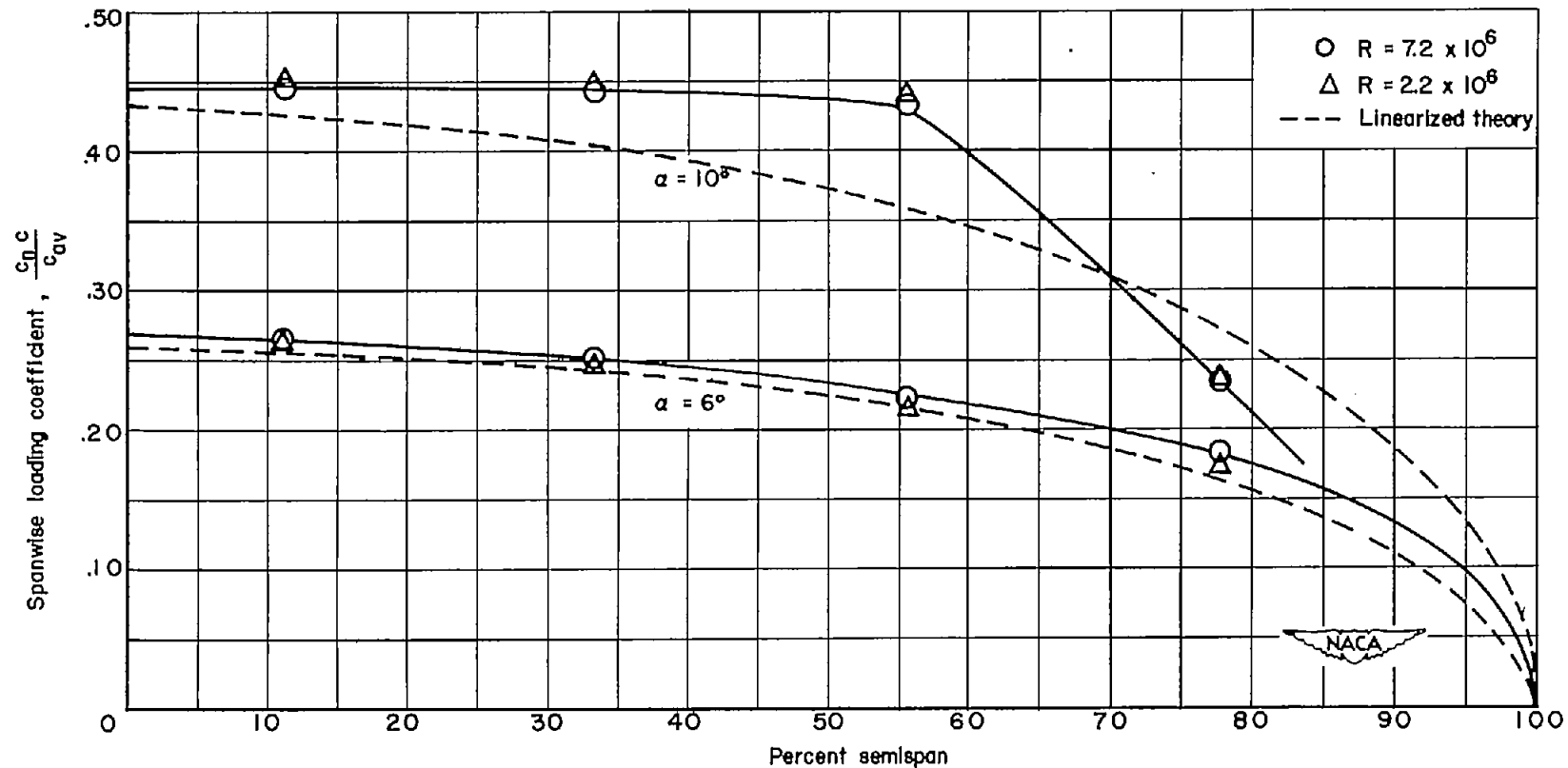
(b) $M = 1.62$.

Figure 14.- Concluded.

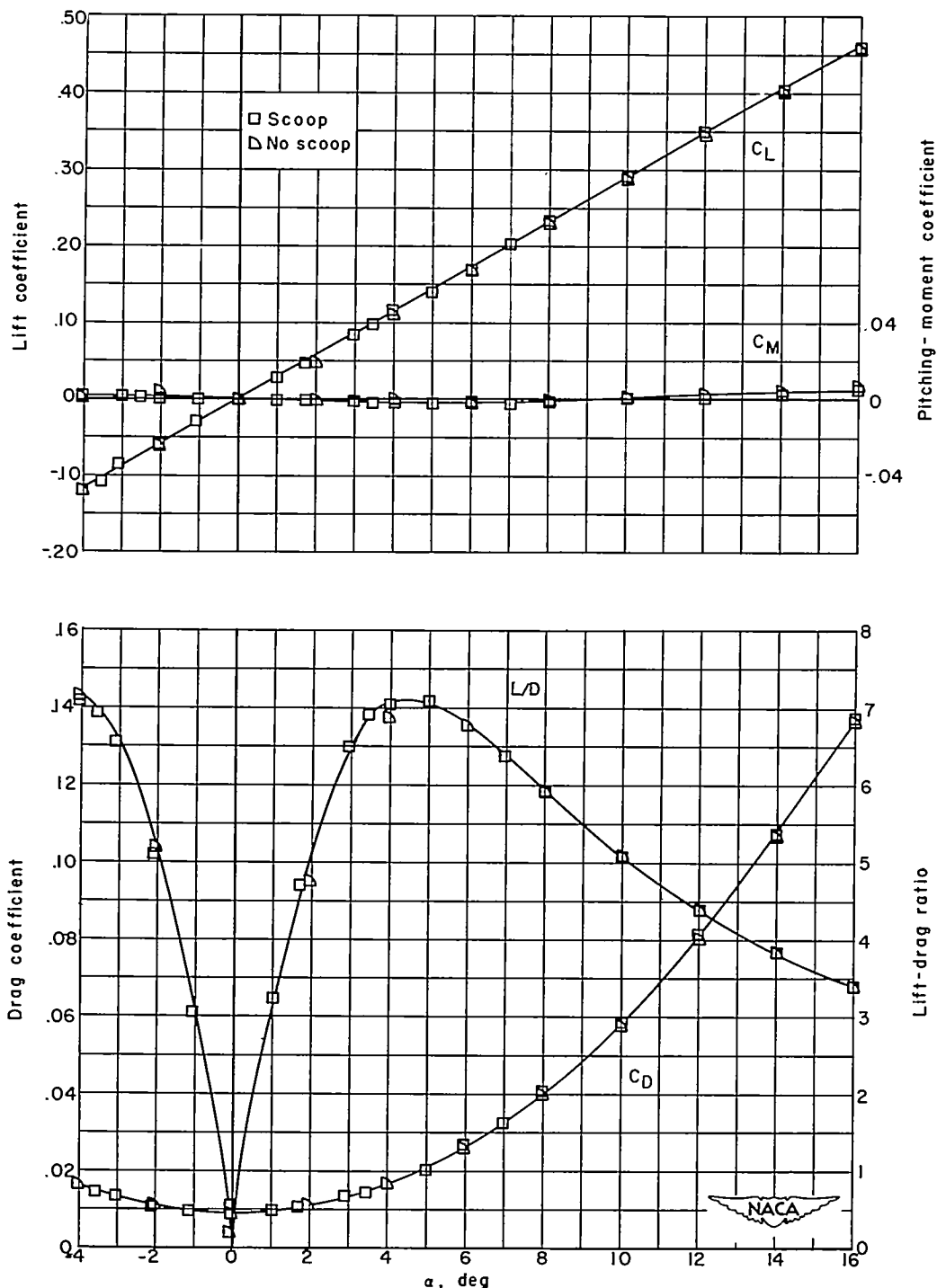
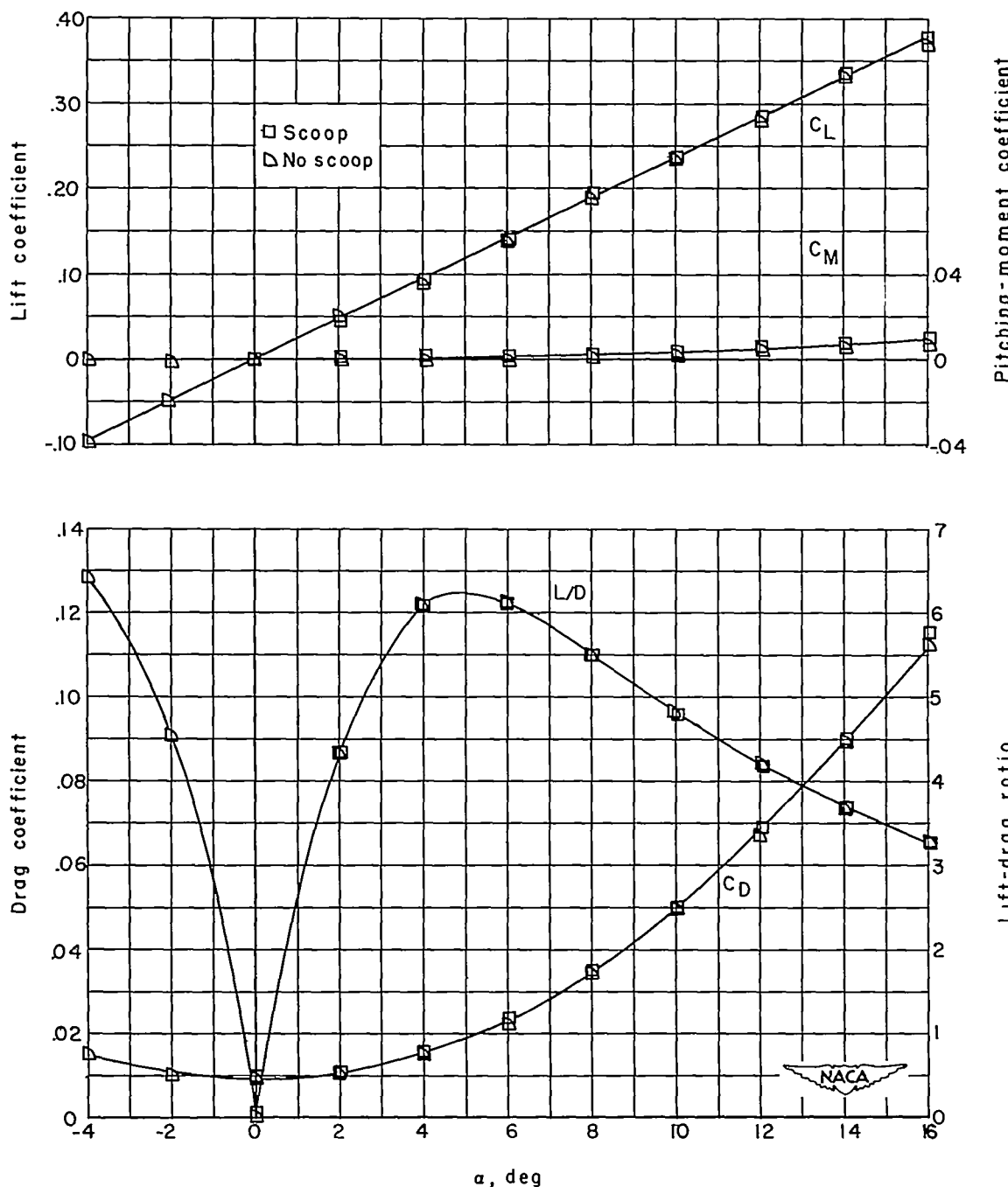
(a) $M = 1.90$.

Figure 15.- Variation of wing aerodynamic characteristics with angle of attack showing the effects of testing with and without a boundary-layer scoop. $R = 18.4 \times 10^6$.



(b) $M = 2.4$; $R = 18.4 \times 10^6$.

Figure 15.- Concluded.

CONFIDENTIAL

NACA RM 153108

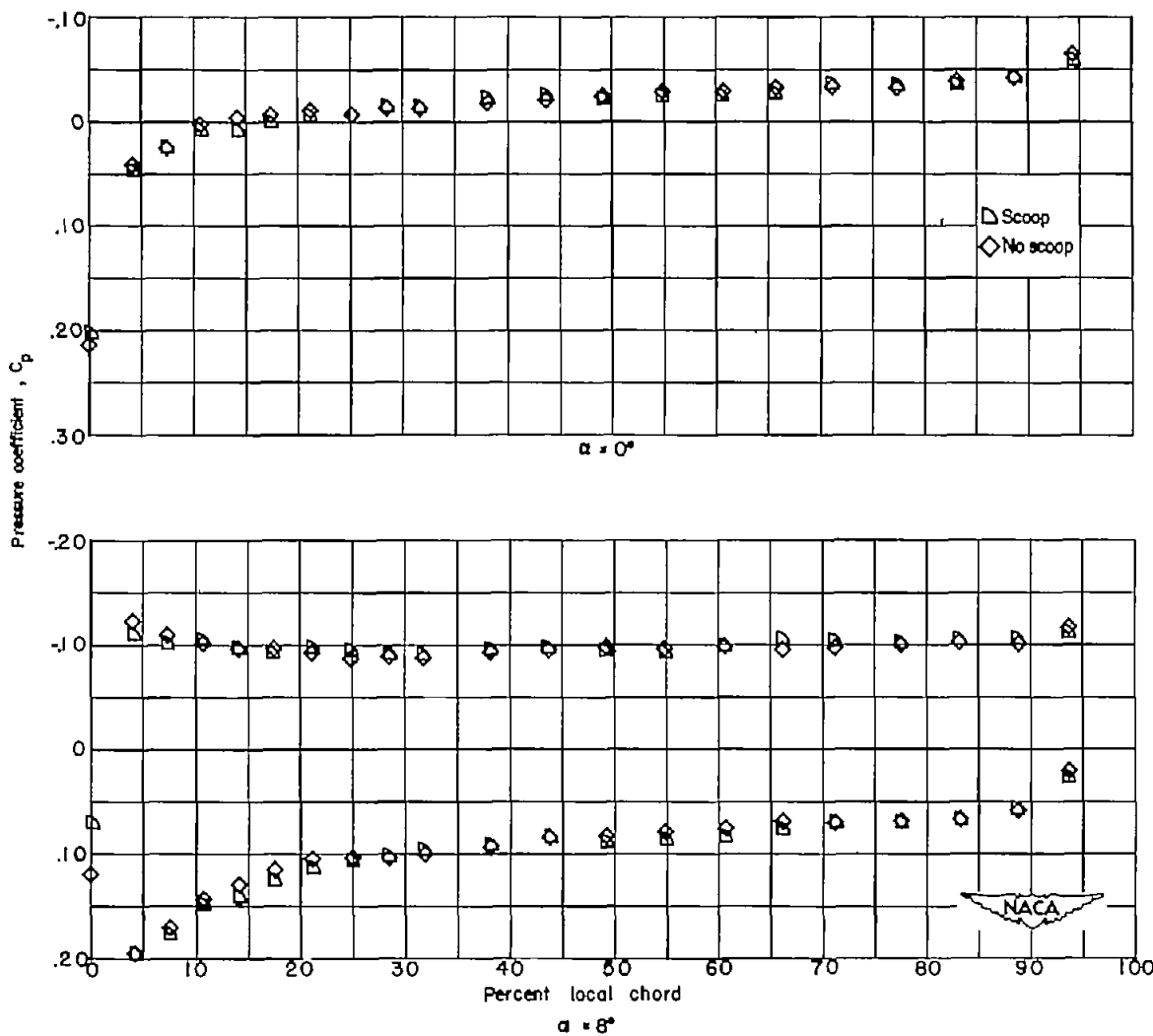
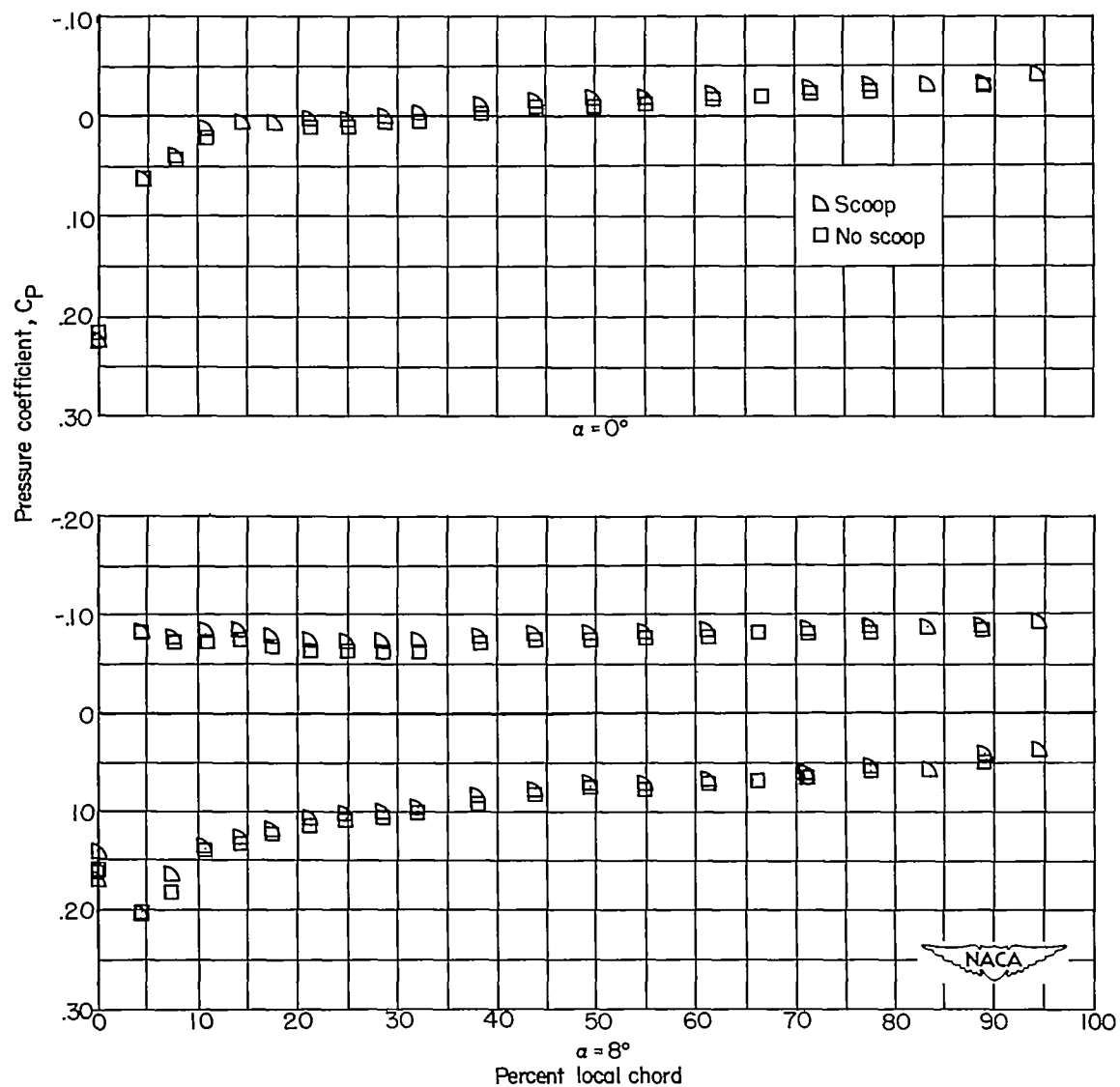


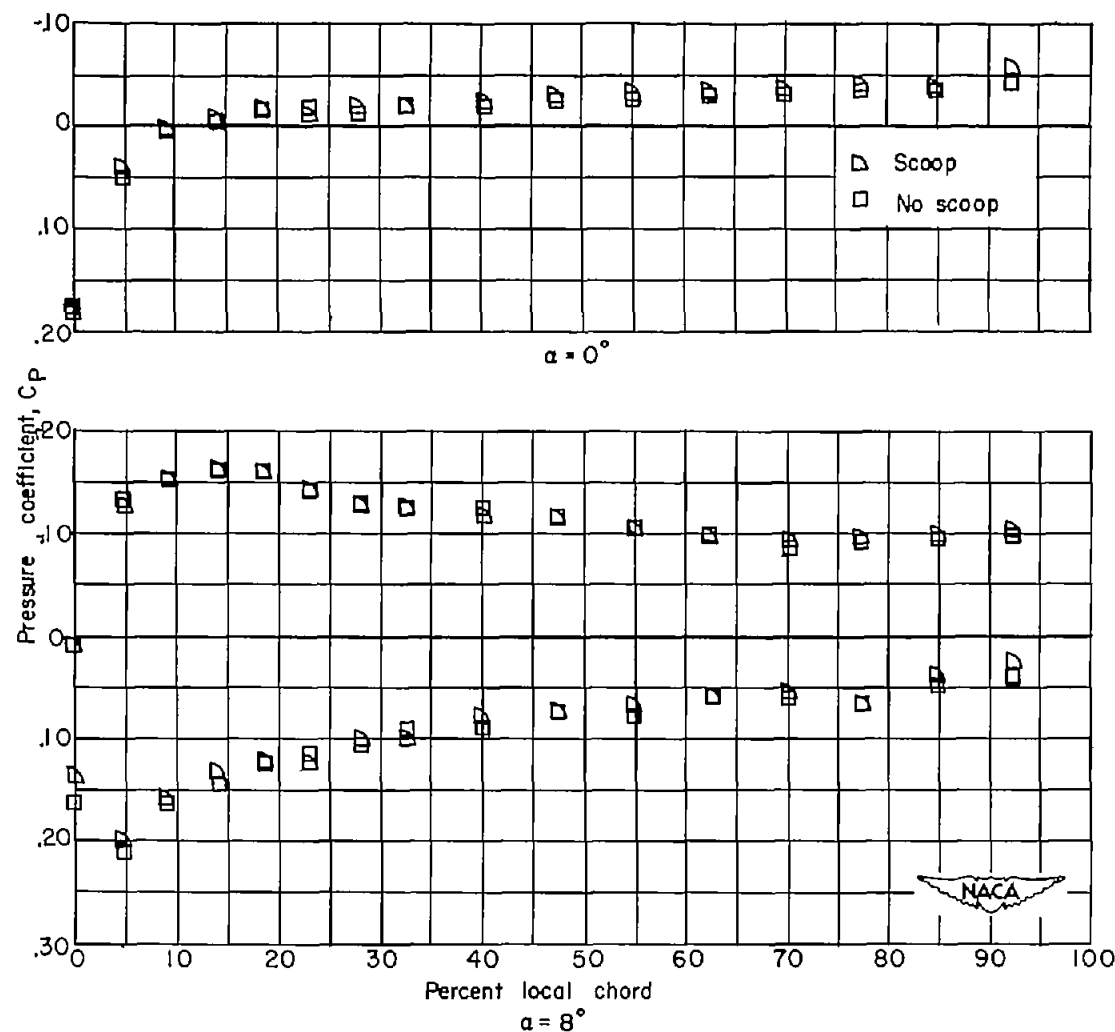
Figure 16.- Comparison of pressure distribution at 11.1-percent semispan station obtained with and without boundary-layer scoop. $M = 1.90$; $R = 18.4 \times 10^6$.

CONFIDENTIAL



(a) 11.1-percent semispan station.

Figure 17.- Comparison of pressure distributions obtained with and without boundary-layer scoop. $M = 2.41$; $R = 18.4 \times 10^6$.



(b) 33.3 semispan station.

Figure 17.- Concluded.